

# Dalton Transactions

Accepted Manuscript

This article can be cited before page numbers have been issued, to do this please use: E. Menéndez-Pedregal, J. Diez, Á. Manteca, J. Sánchez, A. C. Bento, R. García-Navas, F. Mollinedo, P. Gamasa and E. Lastra, *Dalton Trans.*, 2013, DOI: 10.1039/C3DT51160J.



This is an *Accepted Manuscript*, which has been through the RSC Publishing peer review process and has been accepted for publication.

*Accepted Manuscripts* are published online shortly after acceptance, which is prior to technical editing, formatting and proof reading. This free service from RSC Publishing allows authors to make their results available to the community, in citable form, before publication of the edited article. This *Accepted Manuscript* will be replaced by the edited and formatted *Advance Article* as soon as this is available.

To cite this manuscript please use its permanent Digital Object Identifier (DOI®), which is identical for all formats of publication.

More information about *Accepted Manuscripts* can be found in the [Information for Authors](#).

Please note that technical editing may introduce minor changes to the text and/or graphics contained in the manuscript submitted by the author(s) which may alter content, and that the standard [Terms & Conditions](#) and the [ethical guidelines](#) that apply to the journal are still applicable. In no event shall the RSC be held responsible for any errors or omissions in these *Accepted Manuscript* manuscripts or any consequences arising from the use of any information contained in them.

# Antitumor Activity of New Enantiopure Pybox-Ruthenium Complexes

Estefania Menéndez-Pedregal,<sup>a</sup> Josefina Díez,<sup>a</sup> Ángel Manteca,<sup>b</sup> Jesús Sánchez,<sup>b</sup> Ana C. Bento,<sup>c</sup> Rósula García-Navas,<sup>c</sup> Faustino Mollinedo,<sup>c</sup> M. Pilar Gamasa<sup>\*a</sup> and Elena Lastra<sup>\*a</sup>.

Received (in XXX, XXX) Xth XXXXXXXXX 20XX, Accepted Xth XXXXXXXXX 20XX  
DOI: 10.1039/b000000x

## Abstract

New ruthenium complexes containing enantiopure 2,6-bis[4'(*R*)-phenyloxazolin-2'-il-pyridine] ((*R,R*)-Ph-pybox), 2,6-bis[4'(*S*)-isopropylloxazolin-2'-il-pyridine] ((*S,S*)-Pr-pybox) or 2,6-bis[4'(*R*)-isopropylloxazolin-2'-il-pyridine] ((*R,R*)-Pr-pybox) and water soluble 1,3,5-triaza-7-phosphaadamantane (PTA) or N-substituted PTA phosphanes have been synthesized in high yields and fully characterized. The interactions of these compounds with plasmidic DNA and their cytotoxic activity against the human cervical cancer HeLa cell line are reported, pointing out for the first time the different behaviour of ruthenium enantiomers affecting cell cycle in Hela tumor cells.

## Introduction

Search for new therapeutic agents for cancer treatment has lead to an increasing interest for the cytotoxic properties of metal complexes<sup>1</sup> and their mechanisms of action.<sup>2</sup>

In particular, ruthenium-based anticancer drugs have been the subject of active research<sup>3</sup> due in part to the ability of ruthenium to mimic iron in the binding to biological molecules. Thus, ruthenium complexes [ImH][*trans*-RuCl<sub>4</sub>(Im)(DMSO)] (Im = Imidazole) NAMI-A, and [InH][*trans*-RuCl<sub>4</sub>(In)<sub>2</sub>] (In = Indazole) KP1019 have already successfully completed Phase I clinical trials<sup>4</sup> and Ru(II) arene complexes, in particular, arene complexes type [RuCl<sub>2</sub>(η<sup>6</sup>-arene)(PTA)] (RAPTA-complexes) have shown excellent in vitro results.<sup>5</sup>

We have recently reported the synthesis and antitumor activity of a series of water-soluble [tris(pyrazol-1-yl)borate]ruthenium(II) complexes containing PTA and 1-R-PTA phosphanes. These complexes interact with DNA and have an inhibitory effect against human tumor cell lines comparable to anticancer drugs currently used in clinic such as doxorubicin.<sup>6</sup>

In the last years we have been also involved in the synthesis of several transition metal complexes with C<sub>2</sub>-asymmetric tridentate nitrogen ligand pybox (pybox = 2,6-bis[4'(*S*)-isopropylloxazolin-2'-il-pyridine] or 2,6-bis[4'(*R*)-phenyloxazolin-2'-il-pyridine] and their applications in asymmetric catalysis. As part of our ongoing research dealing with groups 8, 9 and 11 metal complexes bearing enantiopure pybox ligands,<sup>7</sup> we have reported the application of ruthenium and iridium complexes in asymmetric transfer hydrogenation of ketones.<sup>8</sup> In particular, we have synthesized enantiopure ruthenium complexes *trans*- and *cis*-[RuCl<sub>2</sub>(L){(*R,R*)-Ph-pybox}] (L = phosphine or phosphite) and found them useful catalysts for asymmetric transfer hydrogenation of ketones (up to 95 % *ee* and very high TOF).<sup>8a</sup>

Since most of the biological molecules are chiral, optical isomers of metallic complexes would interact differently with them and therefore, different biological effects with a chiral molecule as DNA should be observed. Thus, enantiomeric pairs of platinum complexes exhibit different biological activities and different cytotoxicities against different tumor cell lines.<sup>9</sup>

For ruthenium complexes, differences in the behaviour of the enantiomers  $\Lambda$  and  $\Delta$  of octahedral ruthenium complexes have been shown for the cellular uptake<sup>10</sup> as well as for the DNA interaction modes.<sup>11</sup> However, to our knowledge, there are no studies regarding the cytotoxicity of enantiopure ruthenium complexes against tumoral cells.

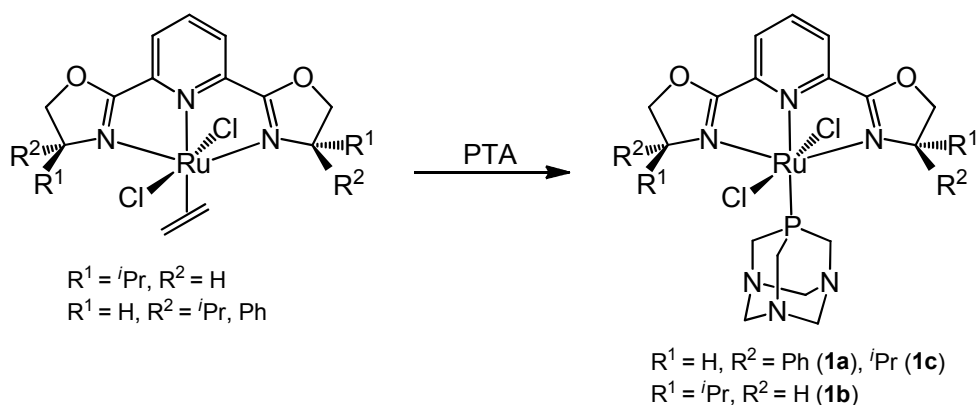
In this scenario we have thought interesting to undertake further studies on the potential biological activity of the ruthenium enantiomer complexes *trans*-[RuCl<sub>2</sub>(L){(*R,R*)-Pr-pybox}] and *trans*-[RuCl<sub>2</sub>(L){(*S,S*)-Pr-pybox}] bearing pybox enantiopure and water-soluble PTA and 1-R-PTA ligands. The PTA ligand<sup>12</sup> has been extensively used to obtain water-soluble transition metal complexes, and many of these compounds harbouring the PTA ligand were in fact described to have interesting antitumor properties.<sup>5</sup>

Here we report the synthesis of novel enantiopure complexes bearing PTA and N-substituted PTA ligands and we analyze their ability to interact with plasmidic DNA as well as their putative antibacterial and antitumor activities. Also, we demonstrate by first time, that some ruthenium enantiomers affect differently cell division in Hela tumor cells.

## Results and discussion

**Synthesis of complexes *trans*-[RuCl<sub>2</sub>{(*R,R*)-Ph-pybox}(PTA)] (1a) and *trans*-[RuCl<sub>2</sub>{(*S,S*)-Pr-pybox}(PTA)] (1b), *trans*-[RuCl<sub>2</sub>{(*R,R*)-Pr-pybox}(PTA)] (1c).** The stereoselective substitution of the ethylene ligand in the

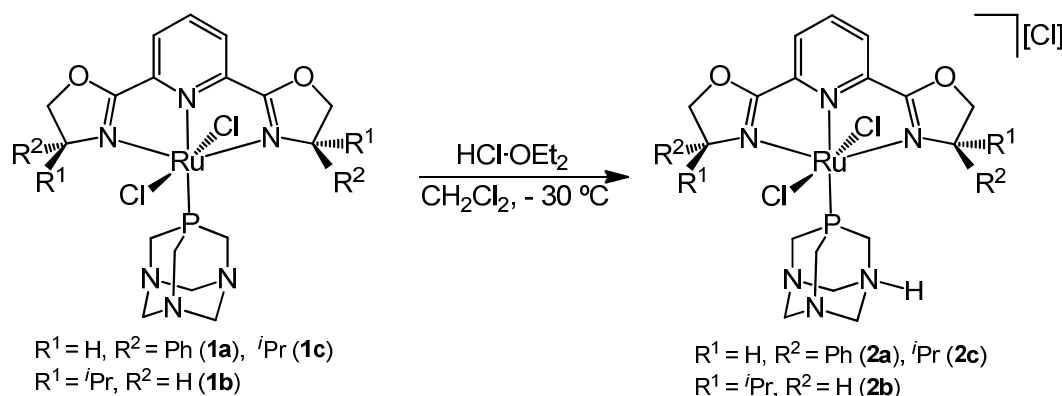
complexes  $trans\text{-}[\text{RuCl}_2(\eta^2\text{-C}_2\text{H}_4)(\text{R-pybox})]$  (R-pybox = (*R,R*)-Ph-pybox, (*S,S*)-*i*Pr-pybox, (*R,R*)-*i*Pr-pybox) by PTA was accomplished in refluxing methanol (for **1a**) or in dichloromethane at room temperature (for **1b** and **1c**) to afford the new complexes **1a–1c** which were isolated as dark purple solids in good yields (90–99 %) (Scheme 1). Complexes **1a–1c** are soluble in water ( $S_{20^\circ\text{C}} = 6.58$  (**1a**) and 31.4 mg/mL (**1b**, **1c**)). These complexes have been characterized by NMR spectroscopy, elemental analysis, and by mass spectra for **1a** and **1b** (see Experimental Section for details). The most significant spectroscopy data are the following: (i) The  $^{31}\text{P}\{^1\text{H}\}$  NMR spectra of these complexes show a singlet resonance at  $\delta = -44.3$  (**1a**) and  $-41.0$  ppm (**1b**, **1c**). (ii) A single set of signals was observed for the pybox ligands in the  $^{13}\text{C}\{^1\text{H}\}$  NMR spectra of complexes **1a**, **1b** and **1c** that is fully consistent with the presence of a  $C_2$  symmetry axis as in the case of their precursor complexes.<sup>13</sup> This evidence implies that the PTA ligand and the pyridine group are in a *trans* arrangement. (iii) The methylene hydrogens  $\text{NCH}_2\text{N}$  of the PTA ligand for complex **1a** appear at 4.33 and 4.06 ppm as AB spin systems ( $J_{\text{H}_\text{A}\text{H}_\text{B}} = 13$  Hz) (in the case of complexes **1b**, **1c** the signals for the  $\text{NCH}_2\text{N}$  (PTA) and  $\text{OCH}_2$  (pybox) groups are overlapped). The  $\text{NCH}_2\text{P}$  hydrogen atoms appear as a CD spin system at 3.60 and 3.52 ppm ( $J_{\text{H}_\text{C}\text{H}_\text{D}} = 15$  Hz) for complex **1a** and as a multiplet at 4.56 ppm for complexes **1b** and **1c**. These data are consistent with those reported for ruthenium complexes containing the PTA ligand.<sup>6,14</sup> The methylene groups of the PTA ligand are found in the  $^{13}\text{C}\{^1\text{H}\}$  NMR spectra as doublets at 72.9 ppm ( $^3J_{\text{CP}} = 6$  Hz) ( $\text{NCH}_2\text{N}$ ) and 52.2 ppm ( $J_{\text{CP}} = 11$  Hz) ( $\text{NCH}_2\text{P}$ ) for complex **1a** and at 73.6 ppm ( $^3J_{\text{CP}} = 6$  Hz) ( $\text{NCH}_2\text{N}$ ) and 53.3 ppm ( $J_{\text{CP}} = 12$  Hz) ( $\text{NCH}_2\text{P}$ ) for complexes **1b**, **1c**.



Scheme 1

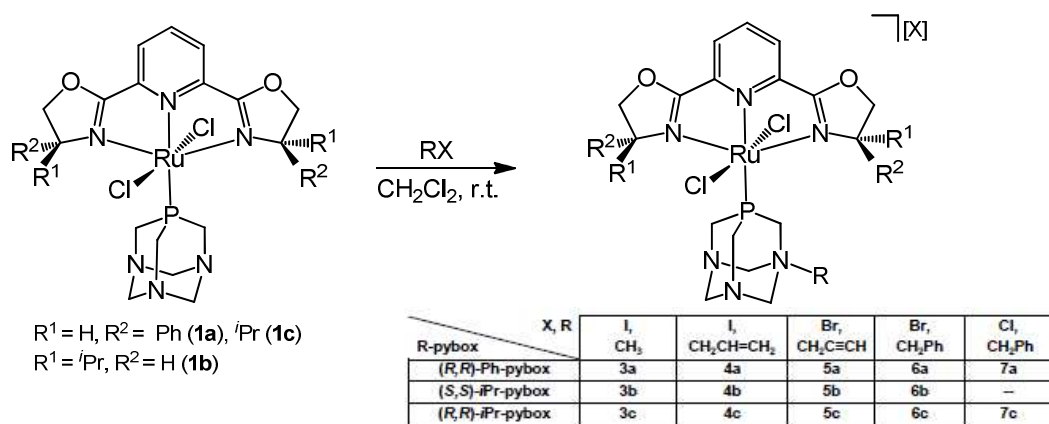
**Reaction of  $trans\text{-}[\text{RuCl}_2(\text{R-pybox})(\text{PTA})]$  (R-pybox = (*R,R*)-Ph-pybox, (*S,S*)-*i*Pr-pybox, (*R,R*)-*i*Pr-pybox) with  $\text{HCl}\cdot\text{OEt}_2$ : Synthesis of complexes  $trans\text{-}[\text{RuCl}_2\{(\text{R},\text{R})\text{-Ph-pybox}\}(1\text{-H-PTA})][\text{Cl}]$  (**2a**),  $trans\text{-}[\text{RuCl}_2\{(\text{S},\text{S})\text{-iPr-pybox}\}(1\text{-H-PTA})][\text{Cl}]$  (**2b**) and  $trans\text{-}[\text{RuCl}_2\{(\text{R},\text{R})\text{-iPr-pybox}\}(1\text{-H-PTA})][\text{Cl}]$  (**2c**).** Addition of an equimolecular amount of  $\text{HCl}\cdot\text{OEt}_2$  (diethyl ether solution, 2M) to a solution of the complexes  $trans\text{-}[\text{RuCl}_2(\text{R-pybox})(\text{PTA})]$  (R-pybox = (*R,R*)-Ph-pybox, (*S,S*)-*i*Pr-pybox, (*R,R*)-*i*Pr-pybox) in dichloromethane at  $-30^\circ\text{C}$  gives rise to the protonation of one of the nitrogen atoms of the coordinated PTA ligand to afford complexes **2a–2c** which were isolated in high yield (80–86 %) (Scheme 2). Complexes **2a–c** show low conductivity values in acetone<sup>15</sup> ( $12\text{--}17\text{ S cm}^2\text{ mol}^{-1}$ ), indicating that the cationic complex makes a tight ionic couple with  $\text{Cl}^-$  in acetone solution. The results are in accordance with the X-ray structure data of complex **2a** for which an hydrogen bond between the H of ammonium group of 1-H-PTA ligand and the chloride is found (see below).

Characteristic features of the spectroscopic data are the following: (i) The  $^{31}\text{P}\{^1\text{H}\}$  NMR spectra exhibit a singlet signal at  $-27.9$  ppm (**2a**) and  $-24.9$  ppm (**2b**, **2c**) which is clearly lower-field shifted in relation with the value found for the precursor complexes ( $-44.3$  ppm for **1a** and  $-41.0$  for **1b**, **1c**).<sup>6a,16</sup> (ii) The signals observed for the pybox ligands in the  $^{13}\text{C}\{^1\text{H}\}$  NMR spectra of complexes **2a–2c** are consistent with the presence of a  $C_2$  symmetry axis thus indicating that the PTA modified ligand and the pyridine group maintain the *trans* arrangement of their precursors. (iii) The NMR spectra show characteristic signals for the H-PTA ligand. Thus, the  $^1\text{H}$  NMR spectra show two broad signals for the hydrogen atoms of the  $\text{NCH}_2\text{N}$  groups of the H-PTA ligand at 4.56 (overlapped with  $\text{OCH}_2$  protons) and 4.18 ppm (**2a**), 4.99 and 4.83 (overlapped with the signals of the  $\text{OCH}_2$  protons) ppm (**2b**, **2c**) and broad signals for the  $\text{NCH}_2\text{P}$  protons at 3.60, 3.46 ppm (**2a**) and 4.60 ppm (**2b**, **2c**). The methylene of the H-PTA ligand resonate in the  $^{13}\text{C}\{^1\text{H}\}$  NMR at 71.4 ppm (**2a**) and 72.1 ppm (**2b**, **2c**) for  $\text{NCH}_2\text{N}$  group and at 49.9 ppm (**2a**) and 53.4 ppm (**2b**, **2c**) for the  $\text{NCH}_2\text{P}$  group. The signals for the carbons of the  $\text{NCH}_2\text{N}$  (**2a,2b**) and  $\text{NCH}_2\text{P}$  (**2a**) groups are higher-field shifted ( $> 1$  ppm) in relation with those found for the precursor complexes **1a** and **1b** (see above).



Scheme 2

**Reaction of *trans*-[RuCl<sub>2</sub>(R-pybox)(PTA)]** (R-pybox = (*R,R*)-Ph-pybox, (*S,S*)-*i*Pr-pybox, (*R,R*)-*i*Pr-pybox) with organic halides: **Synthesis of the complexes *trans*-[RuCl<sub>2</sub>(R-pybox)(1-R-PTA)][X]** (R-pybox = (*R,R*)-Ph-pybox; X = I, R = CH<sub>3</sub> (3a), CH<sub>2</sub>CH=CH<sub>2</sub> (4a), X = Br, R = CH<sub>2</sub>C≡CH (5a), CH<sub>2</sub>Ph (6a), X = Cl, R = CH<sub>2</sub>Ph (7a). R-pybox = (*S,S*)-*i*Pr-pybox; X = I, R = CH<sub>3</sub> (3b), CH<sub>2</sub>CH=CH<sub>2</sub> (4b), X = Br, R = CH<sub>2</sub>C≡CH (5b), CH<sub>2</sub>Ph (6b). R-pybox = (*R,R*)-*i*Pr-pybox; X = I, R = CH<sub>3</sub> (3c), CH<sub>2</sub>CH=CH<sub>2</sub> (4c), X = Br, R = CH<sub>2</sub>C≡CH (5c), CH<sub>2</sub>Ph (6c), X = Cl, R = CH<sub>2</sub>Ph (7c). The reaction of complexes *trans*-[RuCl<sub>2</sub>(R-pybox)(PTA)] (R-pybox = (*R,R*)-Ph-pybox, (*S,S*)-*i*Pr-pybox, (*R,R*)-*i*Pr-pybox,) with organic halides (RX, R = methyl, allyl, propargyl, benzyl) in dichloromethane at room temperature leads to the alkylation of one of the nitrogen atoms of the PTA ligand affording the new complexes **3a–7c** containing the 1-alkyl-3,5-diaza-1-azonia-7-phosphaadamantane (1-R-PTA) ligand (Scheme 3). These complexes are isolated in 60–97 % yields. The solubility of these complexes in H<sub>2</sub>O (293 K) is in the range of 2.45–11.49 mg/mL. The most remarkable features for these complexes are the following: (i) The phosphorous atom of the R-PTA ligand resonates in the <sup>31</sup>P{<sup>1</sup>H} NMR spectra at significantly lower field (δ = 13.7 to –18.4 ppm) than the corresponding precursor complexes. (ii) The <sup>1</sup>H NMR signals have been assigned through COSY HH, HSQC and HMBC experiments and are in agreement with the proposed structures (see Experimental Section). (iii) The single set of signals observed for the pybox ligands in the <sup>13</sup>C{<sup>1</sup>H} NMR spectra of complexes **3a–7c** are consistent with the presence of a C<sub>2</sub> symmetry axis as in the case of their precursor complexes. (iv) While the NCH<sub>2</sub>N and NCH<sub>2</sub>P groups of complexes **1a–1c** display typical AB and CD spin systems, those of complexes **3a–7c** appear as complex multiplets in the ranges of 5.95–2.91 ppm (for Ph-pybox-containing complexes) and 6.31–4.12 ppm (for *i*Pr-pybox-containing complexes). (v) The <sup>1</sup>H and <sup>13</sup>C{<sup>1</sup>H} NMR spectra also show the expected signals for the methyl, allyl, propargyl and benzyl substituents of PTA.



Scheme 3

**Crystal structure of the complexes *trans*-[RuCl<sub>2</sub>{(*S,S*)-*i*Pr-pybox}(PTA)] (1b), *trans*-[RuCl<sub>2</sub>{(*R,R*)-Ph-pybox}(1-H-PTA)][Cl] (2a) and *trans*-[RuCl<sub>2</sub>{(*S,S*)-*i*Pr-pybox}(1-CH<sub>3</sub>-PTA)][I] (3b).** Slow diffusion of hexane into a solution of **1b** or **3b** in dichloromethane allowed us to collect suitable crystals for the X-ray diffraction studies. Crystals suitable for the X-ray study of **2a** were obtained by diffusion of diethyl ether into a saturated solution of this complex in dichloromethane. The asymmetric unit of complex **2a** consists of one molecule of *trans*-[RuCl<sub>2</sub>{(*R,R*)-Ph-pybox}(1-H-PTA)][Cl] and one molecule of dichloromethane (2a·CH<sub>2</sub>Cl<sub>2</sub>). ORTEP type representations of complex **1b** and the cation complex *trans*-[RuCl<sub>2</sub>{(*S,S*)-*i*Pr-pybox}(1-Me-PTA)]<sup>+</sup> and a POV\_Tay drawing of complex

**2a**·CH<sub>2</sub>Cl<sub>2</sub> are shown in Figures 1–3 and selected bonding data are listed in Table 1. The structures exhibit a distorted octahedral geometry around the ruthenium atom which is bonded to the three nitrogen atoms of 'Pr-pybox ligand, the phosphorous atom of PTA (for **1b**), 1-H-PTA (for **2a**) or 1-Me-PTA (for **3b**) ligands and two chlorine atoms (Figures 1–3). The chlorine atoms are located in a *trans* disposition with an Cl(1)–Ru–Cl(2) angle of 177.20(5) (for **1b**), 177.42(8) (for **2a**·CH<sub>2</sub>Cl<sub>2</sub>) and 178.09(10) (for **3b**) deg. The Ru–N(4), Ru–N(5) and Ru–N(6) distances as well as the N–Ru–N bond angles fall in the range observed for other related complexes (see Table 1).<sup>17</sup> The N(5)–Ru–P(1) angle is close to the linearity (178.41(9) (**1b**), 178.6(2) (**2a**), 176.6(2) (**3b**) deg) and the Ru–P(1) distances are in the range of 2.255(2) to 2.3089(9) Å.

In complex **2a**, the N(1)–H(1N) distance has a value of 0.84(18) Å in agreement with the distance values found in the literature for this type of bonds.<sup>18</sup> The structure reveals also the existence of a hydrogen bond between the H(1N) atom and a chloride anion. The H(1N)–Cl bond distances (2.26(17) Å) and the N(1)–H(1N)···Cl angle (156(15) deg) are in accord with this type of binding.<sup>18</sup> For complex **3b**, the distance C(7)–N(1) in the 1-Me-PTA ligand is 1.486(12) Å. These complexes **1b**, **2a**·CH<sub>2</sub>Cl<sub>2</sub>, **3b** present very similar structures with the same stereochemistry, the pyridine nitrogen of the pybox ligand and the PTA, H-PTA and Me-PTA ligands being always in a *trans* arrangement.

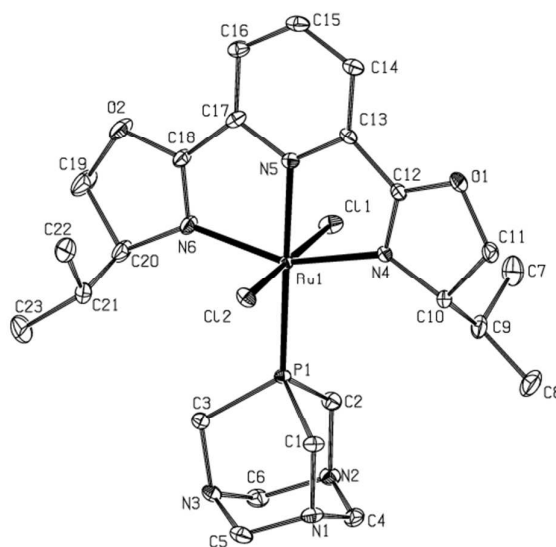


**Figure 1.** An ORTEP type drawing of complex **1b** showing atom-labeling scheme. Thermal ellipsoids are shown at 20 % probability. Hydrogen atoms are omitted for clarity.

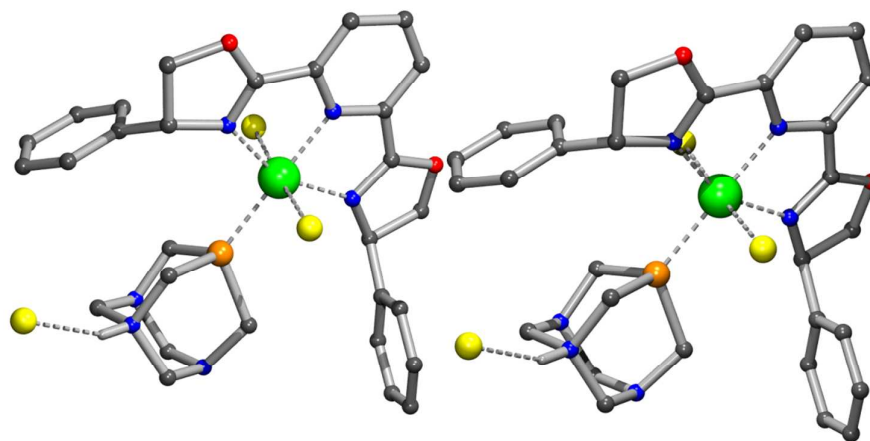


**Figure 2.** A POV-Ray drawing of complex **2a**·CH<sub>2</sub>Cl<sub>2</sub> showing atom-labeling scheme. Hydrogen atoms, except N(1)–H(1N), and solvent molecule are omitted for clarity.

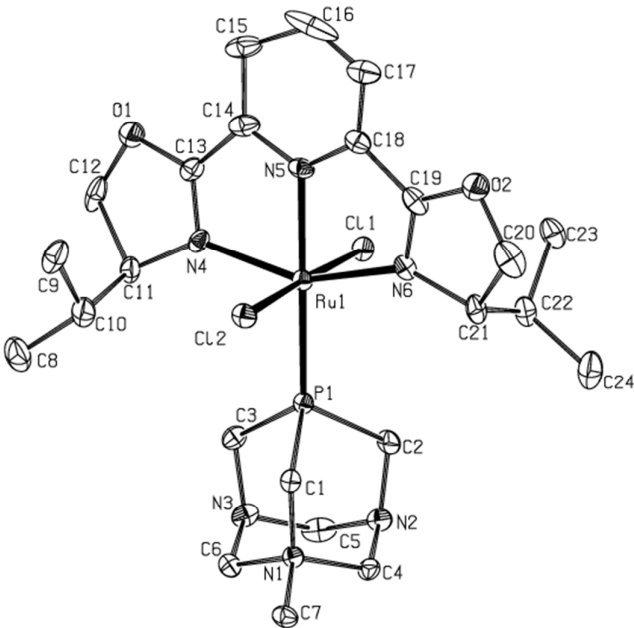


**Figure 3.** An ORTEP type drawing of the cation of complex *trans*-[RuCl<sub>2</sub>{(S,S)-Pr-pybox}(1-Me-PTA)][I] (**3b**) showing atom-labeling scheme. Thermal ellipsoids are shown at 20 % probability. Hydrogen atoms and I<sup>-</sup> anion are omitted for clarity.



**Table 1.** Selected Bond Distances (Å) and Angles (deg) for Complexes **1b**, **2a**·CH<sub>2</sub>Cl<sub>2</sub> and **3b**

Selected Bond Distances (Å) and Angles (deg) for Complex <b>1b</b>			
Bond	Distance	Bond	Distance
Ru–N(4)	2.076(3)	Ru–Cl(1)	2.3905(11)
Ru–N(5)	2.022(4)	Ru–Cl(2)	2.4041(10)
Ru–N(6)	2.075(4)	Ru–P(1)	2.3100(14)
Angle	Value	Angle	Value
N(4)–Ru–P(1)	102.97(11)	N(6)–Ru–Cl(2)	92.68(12)
N(5)–Ru–P(1)	178.40(10)	P(1)–Ru–Cl(1)	91.48(4)
N(6)–Ru–P(1)	102.55(13)	P(1)–Ru–Cl(2)	89.79(4)
N(4)–Ru–Cl(1)	90.32(10)	N(4)–Ru–N(6)	154.47(16)
N(5)–Ru–Cl(1)	86.92(10)	N(5)–Ru–N(6)	77.58(17)
N(6)–Ru–Cl(1)	89.41(13)	N(4)–Ru–N(5)	76.92(15)
N(4)–Ru–Cl(2)	87.04(10)	Cl(1)–Ru–Cl(2)	177.27(5)
N(5)–Ru–Cl(2)	91.80(10)		
Selected Bond Distances (Å) and Angles (deg) for Complex <b>2a</b> ·CH <sub>2</sub> Cl <sub>2</sub>			
Bond	Distance	Bond	Distance
Ru–N(4)	2.086(5)	Ru–Cl(1)	2.402(2)
Ru–N(5)	2.029(6)	Ru–Cl(2)	2.396(2)
Ru–N(6)	2.094(6)	Ru–P(1)	2.286(2)
N(1)–H(1N)	0.87(17)	H(1N)···Cl	2.24(16)
Angle	Value	Angle	Value
N(4)–Ru–P(1)	102.59(16)	N(6)–Ru–Cl(2)	94.11(19)
N(5)–Ru–P(1)	178.5(2)	P(1)–Ru–Cl(1)	94.43(7)
N(6)–Ru–P(1)	102.37(18)	P(1)–Ru–Cl(2)	88.07(7)
N(4)–Ru–Cl(1)	92.48(18)	N(4)–Ru–N(6)	155.0(2)
N(5)–Ru–Cl(1)	87.0(2)	N(5)–Ru–N(6)	77.5(3)
N(6)–Ru–Cl(1)	84.73(19)	N(4)–Ru–N(5)	77.6(2)
N(4)–Ru–Cl(2)	87.61(18)	Cl(1)–Ru–Cl(2)	177.41(8)
N(5)–Ru–Cl(2)	90.49(19)	N(1)–H(1N)···Cl	154(15)
Selected Bond Distances (Å) and Angles (deg) for Complex <b>3b</b>			
Bond	Distance	Bond	Distance
Ru–N(4)	2.107(6)	Ru–Cl(1)	2.4068(14)
Ru–N(5)	2.041(6)	Ru–Cl(2)	2.4096(14)
Ru–N(6)	2.087(5)	Ru–P(1)	2.2752(17)
N(1)–C(7)	1.483(8)		
Angle	Value	Angle	Value
N(4)–Ru–P(1)	102.20(19)	N(6)–Ru–Cl(2)	88.50(18)
N(5)–Ru–P(1)	176.48(17)	P(1)–Ru–Cl(1)	86.78(6)
N(6)–Ru–P(1)	104.43(18)	P(1)–Ru–Cl(2)	91.69(6)
N(4)–Ru–Cl(1)	89.17(15)	N(4)–Ru–N(6)	153.3(3)
N(5)–Ru–Cl(1)	90.19(15)	N(5)–Ru–N(6)	77.4(3)
N(6)–Ru–Cl(1)	90.66(18)	N(4)–Ru–N(5)	75.9(3)
N(4)–Ru–Cl(2)	92.39(16)	Cl(1)–Ru–Cl(2)	178.01(7)
N(5)–Ru–Cl(2)	91.38(15)		

**Chemical behavior in aqueous solution.** All complexes are water soluble with solubilities,  $S_{293\text{ K}}$  (H<sub>2</sub>O), in the range: 2,45 mg/mL to 31,42 mg/mL. Complexes bearing the ligand <sup>1</sup>Pr-pybox show higher solubilities than those bearing the Ph-pybox. Moreover, the <sup>1</sup>Pr-pybox/PTA complex shows higher solubility than the corresponding protonated complex <sup>1</sup>Pr-pybox/1-H-PTA ( $S_{293\text{ K}}$  (H<sub>2</sub>O): 31,42 and 22,45 mg/mL, respectively).

Stability of all complexes under physiological conditions was tested by heating samples of complexes in phosphate buffer solutions at pH = 7 to 37°C. After 72 hours, no appreciable decomposition was observed by <sup>31</sup>P{<sup>1</sup>H} NMR spectroscopy in any of the complexes tested. The experiments were conducted both in the presence and in absence of oxygen and no significant differences were found.

Conductivity measurements in water ( $5 \cdot 10^{-4}$  M) for complexes **1a-c** confirm that these complexes are neutral in aqueous solution, ruling out potential halide dissociation.

**Electrochemical studies.** The electron transfer properties of selected complexes have been studied by cyclic voltammetry techniques. Cyclic voltammetry (CV) experiments in 0.10 M [Bu<sub>4</sub>N][BF<sub>4</sub>]-dichloromethane solutions containing  $5 \times 10^{-4}$  M of the complex were performed at a platinum electrode. CVs of the complexes *trans*-[RuCl<sub>2</sub>(R-pybox)(PTA)] (R-pybox = (*R,R*)-Ph-pybox (**1a**), (*S,S*)-<sup>1</sup>Pr-pybox (**1b**)), *trans*-[RuCl<sub>2</sub>(R-pybox)(1-H-PTA)][Cl] (R-pybox = (*R,R*)-Ph-pybox (**2a**), R-pybox = (*S,S*)-<sup>1</sup>Pr-pybox (**2b**)), *trans*-[RuCl<sub>2</sub>(R-pybox)(1-R-PTA)][X] (R-pybox = (*R,R*)-Ph-pybox, X = I, R = CH<sub>3</sub> (**3a**), CH<sub>2</sub>CH=CH<sub>2</sub> (**4a**); X = Br, R = CH<sub>2</sub>Ph (**6a**); X = Cl, R = CH<sub>2</sub>Ph (**7a**)). R-pybox = (*S,S*)-<sup>1</sup>Pr-pybox, X = I, R = CH<sub>3</sub> (**3b**), CH<sub>2</sub>CH=CH<sub>2</sub> (**4b**); X = Br, R = CH<sub>2</sub>Ph (**6b**)) show a chemical and electrochemical reversible one-electron oxidation wave that can be assigned to a formal one-electron oxidation at the ruthenium(II) center. The  $E^{\circ}_{1/2}$  for these Ru(III)/Ru(II) systems are shown in Table 2. On the other hand, the

complexes **2a** and **2b** show also one reversible wave (0.247 V (**2a**), 0.144 V (**2b**)) which can be tentatively assigned to complexes **1a,b** generated *in situ* by proton dissociation. In according with the higher electron donating capability of the 'Pr-pybox ligand the ruthenium 'Pr-pybox complexes are oxidized at lower potentials than the Ph-pybox complexes. The values of the  $E^{\circ}_{1/2}$  Ru(III)/Ru(II) (**2a–7a** and **2b–6b** vs **1a** and **1b**) are in accordance with the higher potentials expected for the cationic complexes.

**Table 2.** Cyclic voltammetric data<sup>a</sup> for the ruthenium complexes

Compound	$E^{\circ}_{1/2}/V$
<i>trans</i> -[RuCl <sub>2</sub> {( <i>R,R</i> )-Ph-pybox}(PTA)] ( <b>1a</b> )	0.246
<i>trans</i> -[RuCl <sub>2</sub> {( <i>S,S</i> )-'Pr-pybox}(PTA)] ( <b>1b</b> )	0.138
<i>trans</i> -[RuCl <sub>2</sub> {( <i>R,R</i> )-Ph-pybox}(1-H-PTA)][Cl] ( <b>2a</b> )	0.408
<i>trans</i> -[RuCl <sub>2</sub> {( <i>S,S</i> )-'Pr-pybox}(1-H-PTA)][Cl] ( <b>2b</b> )	0.306
<i>trans</i> -[RuCl <sub>2</sub> {( <i>R,R</i> )-Ph-pybox}(1-CH <sub>3</sub> -PTA)][I] ( <b>3a</b> )	0.467
<i>trans</i> -[RuCl <sub>2</sub> {( <i>S,S</i> )-'Pr-pybox}(1-CH <sub>3</sub> -PTA)][I] ( <b>3b</b> )	0.410
<i>trans</i> -[RuCl <sub>2</sub> {( <i>R,R</i> )-Ph-pybox}(1-CH <sub>2</sub> =CHCH <sub>2</sub> -PTA)][I] ( <b>4a</b> )	0.482
<i>trans</i> -[RuCl <sub>2</sub> {( <i>S,S</i> )-'Pr-pybox}(1-CH <sub>2</sub> =CHCH <sub>2</sub> -PTA)][I] ( <b>4b</b> )	0.471
<i>trans</i> -[RuCl <sub>2</sub> {( <i>R,R</i> )-Ph-pybox}(1-PhCH <sub>2</sub> -PTA)][Cl] ( <b>7a</b> )	0.410
<i>trans</i> -[RuCl <sub>2</sub> {( <i>S,S</i> )-'Pr-pybox}(1-PhCH <sub>2</sub> -PTA)][Br] ( <b>6b</b> )	0.369

<sup>a</sup>All electrochemical measurements were carried out in dichloromethane.

**DNA binding properties and cytotoxicity of ruthenium complexes.** Modification of plasmid electrophoretic mobility is commonly taken as evidence for direct DNA-metal interaction. Alteration of the mobility of SC DNA and/ or open circular DNA (OC) indicates a disturbance of the DNA structure by the ruthenium compounds. Retardation of SC DNA was observed for all the analysed compounds, being the effect in plasmid mobility shift, proportional to the concentrations used and demonstrating that all the analysed compounds are interacting “*in vitro*” with DNA (Figure 4). Despite the fact that modification in plasmid mobility is not a quantitative technique, it is clear that compounds with lower solubilities (**1a**, **2a**, **3a**, **4a**, **5a**, **6a**) were the most effective ones, as all of them showed a dramatic alteration of plasmid mobility at concentrations of 0.1mM (Figure 4a), while the rest of the compounds only had a slightly effect in the plasmid mobility at these concentrations (Figure 4b and 4c). This is specially accentuated for compounds **4a**, **5a** and **6a**, which showed a great effect modifying plasmid mobility at concentrations as lower as 0.05mM (Figure 4a). Further work will be necessary to characterize in detail the biochemical mechanisms behind this behaviour.



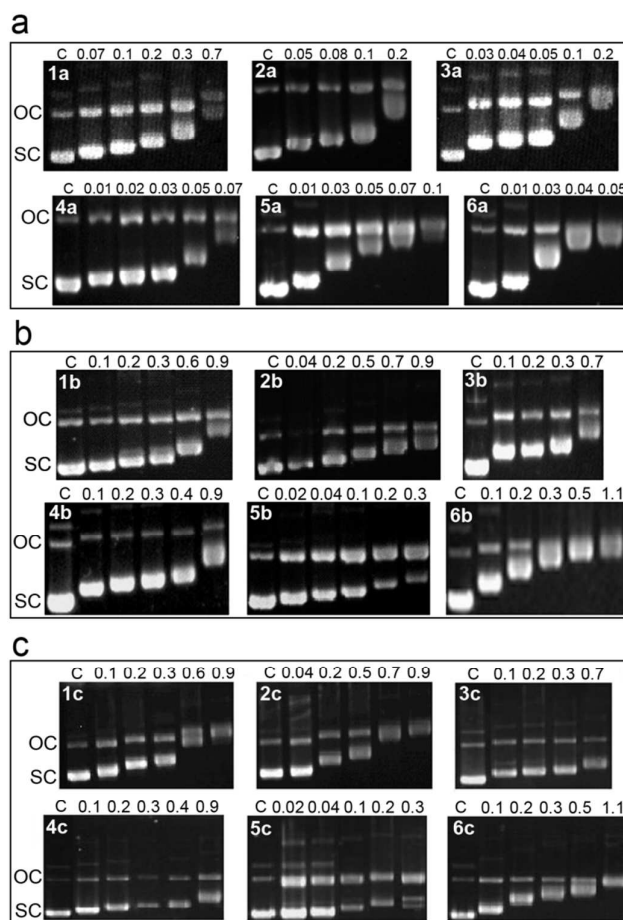


**Figure 4.** DNA mobility shift assay for ruthenium complexes **1a-6a**, **1b-6b**, **1c-6c**. The range of ruthenium complex concentrations used (mM) is indicated (top of the panels). C is the control lane without the ruthenium complex. OC, open circular plasmidic DNA; SC, supercoiled DNA.

A first indication of the “*in vivo*” activity of these novel ruthenium complexes was obtained using the Kirby Bauer diffusion method<sup>19</sup> against six different bacteria (*M. luteus*, *B. subtilis*, *E. coli*, *S. coelicolor*, *S. antibioticus*, and *P. aeruginosa*) and two yeasts (*C. albicans* and *C. parapsilosis*). All the compounds were active against these microorganisms, but they had different intensities of microbial growth inhibition in function of the microorganism tested (See Supplementary Material Figure 1 and Table 1.) The microbial activity of these compounds was comparable to that presented by clinical antibiotics (for instance, 0.045  $\mu\text{g}$  of erythromycin produce a 10 mm inhibition halo against *M. luteus*). However, the antimicrobial activity of these compounds cannot be exploited in clinic because they interact with DNA, and in consequence, their biological effect is not specific for microbes. As previously reported for hydridotris(pyrazolyl)borate ruthenium(II) complexes,<sup>6b</sup> gram positive bacteria (*M. luteus*, *B. subtilis*, *S. coelicolor*, and *S. antibioticus*) were more susceptible to ruthenium compounds than the gram negative ones (*E. coli*, *P. aeruginosa*) or eukaryotic microbes (*C. albicans*, *C. parapsilosis*). This differential sensitivity could be due to differences in bacterial cellular covers (gram negative cell wall consists of at least two layers, whereas the gram-positive cell wall is typically much thicker and consists primarily of a single type of molecule). An impediment in the access of the compounds to cellular DNA might be also the reason for the high resistance observed in yeasts, because in contrast to what happens in bacteria, chromosomal DNA in eukaryotes is protected by the nuclear membrane. Overall, biological factors are affecting the activity of these complexes, a fact that should be considered in order to explore future clinical applications of these compounds.

**Biological activity of ruthenium complexes against human HeLa tumor cell line** We next analyzed the cytotoxic activity of these compounds against the human cervical cancer HeLa cell line. Because several of the compounds to be assayed were colored, the typical colorimetric assays to determine cell proliferation were not reliable. Thus, we analyzed the ability to induce apoptosis in human cervical cancer HeLa cells of compounds **1a-7a**, **1b-6b** and **3c**, **6c** and **7c** by using fluorescence flow cytometry analysis of cell cycle. In a typical experiment, cells were incubated with solutions of different concentrations of the ruthenium complexes for 48 and 72 h and DNA content was analyzed by

fluorescence flow cytometry following DNA staining with propidium iodide (PI). PI fluorescence is proportional to the amount of chromosomal DNA and allows to identify distinct stages of the cell. Cells at the non-division stage only have a copy of chromosomal DNA (phases  $G_0/G_1$ ); after nuclear division they have two copies of chromosomal DNA (phases  $G_2/M$ ); and apoptotic cells show DNA degradation, and have less PI fluorescence than intact cells (sub- $G_0/G_1$  phase). The presence of cells with fragmented DNA (the so-called sub- $G_0/G_1$  cell cycle phase; hypodiploidy) is a well-known indicator of apoptosis.<sup>20</sup> The above compounds did not trigger apoptosis when used at 1, 10 or 100  $\mu\text{M}$  for 24 or 48 h (data not shown). However after 72 h incubation time, all of them showed a rather weak ability to promote apoptosis that could reach about 10% at 100  $\mu\text{M}$  (Table 3). Only compound  $[\text{RuCl}_2(\kappa^3\text{-}N,N,N\text{-}(R,R)\text{-Ph-pybox})(1\text{-PhCH}_2\text{-PTA})][\text{Cl}]$  (**7a**) showed a greater apoptotic activity (21% apoptosis) (Table 3).

Table 3. Induction of apoptosis in HeLa cells by ruthenium complexes

Compound	% Apoptosis (72h)	
	10 $\mu\text{M}$	100 $\mu\text{M}$
$[\text{RuCl}_2\{(R,R)\text{-Ph-pybox}\}(\text{PTA})][\text{Cl}]$ ( <b>1a</b> )	$6.8 \pm 0.8$	$11.3 \pm 1.7$
$[\text{RuCl}_2\{(S,S)\text{-}^i\text{Pr-pybox}\}(\text{PTA})][\text{Cl}]$ ( <b>1b</b> )	$8.0 \pm 1.1$	$8.9 \pm 1.3$
$[\text{RuCl}_2\{(R,R)\text{-Ph-pybox}\}(1\text{-H-PTA})][\text{Cl}]$ ( <b>2a</b> )	$3.3 \pm 0.6$	$3.9 \pm 0.8$
$[\text{RuCl}_2\{(S,S)\text{-}^i\text{Pr-pybox}\}(1\text{-H-PTA})][\text{Cl}]$ ( <b>2b</b> )	$3.8 \pm 0.6$	$7.8 \pm 0.9$
$[\text{RuCl}_2\{(R,R)\text{-Ph-pybox}\}(1\text{-CH}_3\text{-PTA})][\text{I}]$ ( <b>3a</b> )	$8.0 \pm 1.0$	$12.3 \pm 1.9$
$[\text{RuCl}_2\{(S,S)\text{-}^i\text{Pr-pybox}\}(1\text{-CH}_3\text{-PTA})][\text{I}]$ ( <b>3b</b> )	$9.3 \pm 1.0$	$11.4 \pm 1.7$
$[\text{RuCl}_2\{(R,R)\text{-}^i\text{Pr-pybox}\}(1\text{-CH}_3\text{-PTA})][\text{I}]$ ( <b>3c</b> )	$12.4 \pm 1.5$	$13.5 \pm 1.6$
$[\text{RuCl}_2\{(R,R)\text{-Ph-pybox}\}(1\text{-CH}_2=\text{CHCH}_2\text{-PTA})][\text{I}]$ ( <b>4a</b> )	$8.1 \pm 1.3$	$11.2 \pm 1.8$
$[\text{RuCl}_2\{(S,S)\text{-}^i\text{Pr-pybox}\}(1\text{-CH}_2=\text{CHCH}_2\text{-PTA})][\text{I}]$ ( <b>4b</b> )	$6.2 \pm 0.9$	$7.8 \pm 1.1$
$[\text{RuCl}_2\{(R,R)\text{-Ph-pybox}\}(1\text{-HC}\equiv\text{CCH}_2\text{-PTA})][\text{Br}]$ ( <b>5a</b> )	$4.7 \pm 0.7$	$10.6 \pm 1.7$
$[\text{RuCl}_2\{(S,S)\text{-}^i\text{Pr-pybox}\}(1\text{-HC}\equiv\text{CCH}_2\text{-PTA})][\text{Br}]$ ( <b>5b</b> )	$5.5 \pm 0.8$	$12.5 \pm 2.3$
$[\text{RuCl}_2\{(R,R)\text{-Ph-pybox}\}(1\text{-PhCH}_2\text{-PTA})][\text{Br}]$ ( <b>6a</b> )	$9.9 \pm 1.1$	$11.1 \pm 1.3$
$[\text{RuCl}_2\{(S,S)\text{-}^i\text{Pr-pybox}\}(1\text{-PhCH}_2\text{-PTA})][\text{Br}]$ ( <b>6b</b> )	$9.3 \pm 1.5$	$12.5 \pm 2.0$
$[\text{RuCl}_2\{(R,R)\text{-}^i\text{Pr-pybox}\}(1\text{-PhCH}_2\text{-PTA})][\text{Br}]$ ( <b>6c</b> )	$10.2 \pm 1.3$	$14.8 \pm 1.7$
$[\text{RuCl}_2\{(R,R)\text{-Ph-pybox}\}(1\text{-PhCH}_2\text{-PTA})][\text{Cl}]$ ( <b>7a</b> )	$11.0 \pm 1.2$	$21.0 \pm 2.6$
$[\text{RuCl}_2\{(R,R)\text{-}^i\text{Pr-pybox}\}(1\text{-PhCH}_2\text{-PTA})][\text{Cl}]$ ( <b>7c</b> )	$7.8 \pm 0.9$	$13.1 \pm 1.6$

HeLa cells were incubated with 10 and 100  $\mu\text{M}$  of the indicated compounds for 72 h, and then analyzed for cell cycle analysis by flow cytometry. Quantitation of apoptotic cells was determined as the percentage of cells in the sub- $G_0/G_1$  region (hypodiploidy) in cell cycle analysis. Untreated control HeLa cells showed < 3% apoptosis after 72 h incubation. Data shown are means  $\pm$  S.D. of three independent experiments.

Despite data shown in Table 3 indicate a rather poor cytotoxic activity for the above compounds, interestingly a different response was detected for enantiomers  $[\text{RuCl}_2(\kappa^3\text{-}N,N,N\text{-}(S,S)\text{-}^i\text{Pr-pybox})(1\text{-CH}_3\text{-PTA})][\text{I}]$  (**3b**) /  $[\text{RuCl}_2(\kappa^3\text{-}N,N,N\text{-}(R,R)\text{-}^i\text{Pr-pybox})(1\text{-CH}_3\text{-PTA})][\text{I}]$  (**3c**) and  $[\text{RuCl}_2(\kappa^3\text{-}N,N,N\text{-}(S,S)\text{-}^i\text{Pr-pybox})(1\text{-PhCH}_2\text{-PTA})][\text{Br}]$  (**6b**) /  $[\text{RuCl}_2(\kappa^3\text{-}N,N,N\text{-}(R,R)\text{-}^i\text{Pr-pybox})(1\text{-PhCH}_2\text{-PTA})][\text{Br}]$  (**6c**) in relation to their effects on cell cycle. Compounds **3b** and **6b** bearing the ligand  $(S,S)\text{-}^i\text{Pr-pybox}$  did not affect significantly the different phases of cell cycle, while their enantiomers **3c** and **6c** bearing the  $(R,R)\text{-}^i\text{Pr-pybox}$  isomer induced an abundant (up to 58% of the cells) cellular arrest at the  $G_2/M$  cell cycle phase, after 72 h incubation time (Figure 5 and Table 4). This growth arrest led to apoptotic cell death (>20%) after protracted incubation times (>72 h). This is in agreement with the notion that a protracted growth arrest at  $G_2/M$  might lead to cell death through a mechanism not yet well defined.<sup>21</sup> Nevertheless, these results suggest a rather weak antitumor activity for these compounds, irrespectively, of their effects on cell cycle as high drug concentrations and very long incubation times are required to promote cell death in HeLa cells.

Table 4. Percentage of HeLa cells accumulated at the  $G_2/M$  cell cycle phase following treatment with the enantiomers **3b,c** and **6b,c**

Compound	% $G_2/M$	
	48 h	72 h
Control (untreated)	$21.5 \pm 3.2$	$19.8 \pm 3.3$
$[\text{RuCl}_2\{(S,S)\text{-}^i\text{Pr-pybox}\}(1\text{-CH}_3\text{-PTA})][\text{I}]$ ( <b>3b</b> )	$18.0 \pm 2.8$	$11.8 \pm 2.4$
$[\text{RuCl}_2\{(R,R)\text{-}^i\text{Pr-pybox}\}(1\text{-CH}_3\text{-PTA})][\text{I}]$ ( <b>3c</b> )	$43.9 \pm 4.2$	$58.5 \pm 4.8$
$[\text{RuCl}_2\{(S,S)\text{-}^i\text{Pr-pybox}\}(1\text{-PhCH}_2\text{-PTA})][\text{Br}]$ ( <b>6b</b> )	$26.9 \pm 3.1$	$11.7 \pm 2.8$
$[\text{RuCl}_2\{(R,R)\text{-}^i\text{Pr-pybox}\}(1\text{-PhCH}_2\text{-PTA})][\text{Br}]$ ( <b>6c</b> )	$33.9 \pm 3.6$	$46.8 \pm 4.5$

HeLa cells were incubated with 100  $\mu\text{M}$  of the indicated compounds for 72 h, and then analyzed for cell cycle analysis by flow cytometry. Quantitation of the percentage of cells at the  $G_2/M$  cell cycle phase was performed in cell cycle analysis. Data shown are means  $\pm$  S.D. or representative of three independent experiments.

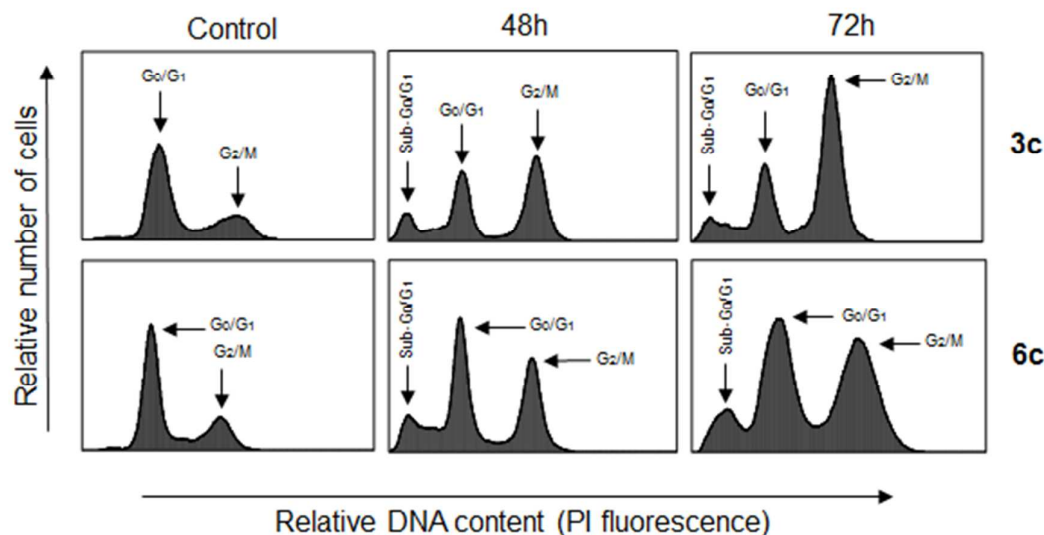


Figure 5. Effects of compounds **3c** and **6c** on cell cycle in HeLa cells. Cells were incubated with 100  $\mu$ M of compounds **3c** and **6c** for 48 and 72 h, and their DNA content was analyzed by fluorescence flow cytometry following staining with propidium iodide (PI). The positions of G<sub>0</sub>/G<sub>1</sub> and G<sub>2</sub>/M peaks are indicated by arrows. The region corresponding to apoptotic cells (sub-G<sub>0</sub>/G<sub>1</sub>) is also indicated. Control untreated cells were run in parallel. Data shown are representative of three separate experiments.

## Experimental

**General** All manipulations were performed under an atmosphere of dry nitrogen using vacuum-line and standard Schlenk techniques. The reagents were obtained from commercial suppliers and used without further purification. Solvents were dried by standard methods and distilled under nitrogen before use. The complexes *trans*-[RuCl( $\mu$ -Cl)( $\eta^6$ -p-cymene)]<sub>2</sub>,<sup>22</sup> [RuCl<sub>2</sub>( $\eta^2$ -C<sub>2</sub>H<sub>4</sub>)( $\kappa^3$ -N,N,N'-Pr-pybox)] and [RuCl<sub>2</sub>( $\eta^2$ -C<sub>2</sub>H<sub>4</sub>)( $\kappa^3$ -N,N,N'-Ph-pybox)],<sup>23</sup> pybox<sup>24</sup> and 1,3,5-triaza-7-phosphatricyclo[3.3.1.1]decane (PTA)<sup>25</sup> ligands were synthesized by reported methods.

The complexes reported in this article have been characterized by NMR spectroscopy and elemental analysis or mass spectra (for **1a**, **1b**, **2b** and **6a**). Infrared spectra were recorded on a Perkin-Elmer 1720-XFT spectrometer. The C, H, N analyses were carried out with a LECO CHNS-TruSpec and a Perkin-Elmer 240-B microanalyzers. Mass spectra (MALDI-TOF) were determined with a Microflex Bruker spectrometer, operating in the positive mode; DCTB was used as the matrix. Electrospray mass spectra (ESI-MS) were recorded on a MicroToF-Q Bruker instrument, operating in the positive mode and using methanol solutions. MALDI-TOF or ESI-MS experiments have been carried out for the precursor complexes **1a** and **1b** as well as for complexes **2b** and **6a** (no satisfactory analysis was obtained for complexes **1b**, **2b** and **6a**). NMR spectra were recorded on Bruker spectrometers (AV400 operating at 400.13 (<sup>1</sup>H), 100.61 (<sup>13</sup>C) and 161.95 (<sup>31</sup>P) MHz or DPX300 operating at 300.13 (<sup>1</sup>H), 75.45 (<sup>13</sup>C) MHz) and 121.49 (<sup>31</sup>P) MHz. DEPT and Bidimensional COSY HH, HSQC and HMBC experiments were carried out for all the compounds. Chemical shifts are reported in parts per million and referenced to TMS or 85% H<sub>3</sub>PO<sub>4</sub> as standards. Coupling constants *J* are given in hertz. The following atom labels have been used for the <sup>1</sup>H and <sup>13</sup>C{<sup>1</sup>H} spectroscopic data of the pybox ligands. Spectroscopic data for complexes **2c-6c** bearing the (*R,R*)-*i*Pr-pybox ligand can be found as supplementary material.

**Synthesis of complex *trans*-[RuCl<sub>2</sub>{(*R,R*)-Ph-pybox}(PTA)] (**1a**).** To a solution of the complex *trans*-[RuCl<sub>2</sub>( $\eta^2$ -C<sub>2</sub>H<sub>4</sub>){(*R,R*)-Ph-pybox}] (0.398 g, 0.70 mmol) in methanol (35 mL), an equivalent of the phosphine PTA (0.111 g, 0.709 mmol) was added and the resulting mixture was heated at reflux temperature for 3.5 hours. The solution was concentrated to ca. 2 mL and the addition of diethyl ether (50 mL) afforded a dark purple solid precipitate. Solvents were decanted and the solid residue was washed with diethyl ether (2 x 15 mL) and dried under vacuum. Yield: 0.425 g, 87%. S<sub>293 K</sub> (H<sub>2</sub>O): 6.58 mg/mL. Anal. Calcd. for C<sub>29</sub>H<sub>31</sub>Cl<sub>2</sub>N<sub>6</sub>O<sub>2</sub>PRu: C, 49.86; H, 4.47; N, 12.03. Found: C, 49.29; H, 4.28; N, 11.81. MALDI-TOF-MS (DCTB): *m/z* = 698.2 [RuCl<sub>2</sub>(Ph-pybox)(PTA)]<sup>+</sup> (47 %), 663.2 [RuCl(Ph-pybox)(PTA)]<sup>+</sup> (100 %). <sup>1</sup>H NMR (400.13 MHz, CD<sub>2</sub>Cl<sub>2</sub>, 298 K)  $\delta$  7.98 (m, 3H, H<sup>3,4,5</sup> C<sub>5</sub>H<sub>3</sub>N), 7.38 (m, 10H, Ph), 5.22 (m, 2H, OCH<sub>2</sub>), 5.12 (m, 2H, CHPh), 4.58 (m, 2H, OCH<sub>2</sub>), 4.33 (AB spin system, *J*<sub>HAB</sub> = 13 Hz, 3H, NCH<sub>2</sub>N), 4.06 (AB spin system, *J*<sub>HAB</sub> = 13 Hz, 3H, NCH<sub>2</sub>N), 3.60 (CD spin system, *J*<sub>HCHD</sub> = 15 Hz, 3H, NCH<sub>2</sub>P), 3.52 (CD spin system, 3H, *J*<sub>HCHD</sub> = 15 Hz, NCH<sub>2</sub>P) ppm. <sup>13</sup>C{<sup>1</sup>H} NMR (100.61 MHz, CD<sub>2</sub>Cl<sub>2</sub>, 298 K)  $\delta$  167.4 (s, OCN), 147.8 (s, C<sup>2,6</sup> C<sub>5</sub>H<sub>3</sub>N), 139.3 (s, C<sup>ipso</sup> Ph), 132.9 (s, C<sup>4</sup> C<sub>5</sub>H<sub>3</sub>N), 128.9, 128.4, 127.8 (3s, Ph), 123.7 (s, C<sup>3,5</sup> C<sub>5</sub>H<sub>3</sub>N), 78.7 (s, OCH<sub>2</sub>), 72.9 (d, <sup>3</sup>*J*<sub>CP</sub> = 6 Hz, NCH<sub>2</sub>N), 71.0 (s, CHPh), 52.2 (d, *J*<sub>CP</sub> = 11 Hz, NCH<sub>2</sub>P) ppm. <sup>31</sup>P{<sup>1</sup>H} NMR (161.95 MHz, CD<sub>2</sub>Cl<sub>2</sub>, 298 K)  $\delta$  -44.3 (s) ppm.

**Synthesis of complexes *trans*-[RuCl<sub>2</sub>{(*S,S*)-*i*Pr-pybox}(PTA)] (**1b**) and *trans*-[RuCl<sub>2</sub>{(*R,R*)-*i*Pr-pybox}(PTA)] (**1c**)** To a solution of the complex *trans*-[RuCl<sub>2</sub>( $\eta^2$ -C<sub>2</sub>H<sub>4</sub>){(*S,S*)-*i*Pr-pybox}] or *trans*-[RuCl<sub>2</sub>( $\eta^2$ -C<sub>2</sub>H<sub>4</sub>){(*R,R*)-*i*Pr-

pybox)}] (0.351 g, 0.70 mmol) in dichloromethane (20 mL), the phosphine PTA (0.110 g, 0.702 mmol) was added and the resulting mixture was stirred at room temperature for 9 hours. The solution was concentrated to ca. 3 mL and the addition of an hexane-diethyl ether mixture (50 mL, 2:1) afforded a dark purple solid precipitate. Solvents were decanted and the solid residue was washed with hexane (2 x 15 mL) and dried under vacuum.

**1b** Yield: 0.402 g, 91%.  $S_{293\text{ K}}$  ( $\text{H}_2\text{O}$ ): 31.42 mg/mL. Anal. Calcd. for  $\text{C}_{23}\text{H}_{35}\text{Cl}_2\text{N}_6\text{O}_2\text{PRu}$ : C, 43.81; H, 5.60; N, 13.33. Found: C, 42.86; H, 5.53; N, 12.72. MALDI-TOF-MS (DCTB):  $m/z = 632.2$   $[\text{RuCl}_2(\text{Pr-pybox})(\text{PTA})+\text{I}]^+$  (100 %), 595.2  $[\text{RuCl}(\text{Pr-pybox})(\text{PTA})]^+$  (58 %).  $^1\text{H}$  NMR (400.13 MHz,  $\text{CD}_2\text{Cl}_2$ , 298 K)  $\delta$  7.88 (m, 3H,  $\text{H}^{3,4,5}$   $\text{C}_5\text{H}_3\text{N}$ ), 4.85–4.70 (m, 10H,  $\text{OCH}_2$ ,  $\text{NCH}_2\text{N}$ ), 4.56 (m, 6H,  $\text{NCH}_2\text{P}$ ), 3.95 (m, 2H,  $\text{CH}^i\text{Pr}$ ), 2.27 (m, 2H,  $\text{CHMe}_2$ ), 1.07 (d,  $^3J_{\text{HH}} = 7.6$  Hz, 6H,  $\text{CHMe}_2$ ), 0.72 (d,  $^3J_{\text{HH}} = 6.4$  Hz, 6H,  $\text{CHMe}_2$ ) ppm.  $^{13}\text{C}\{^1\text{H}\}$  NMR (100.61 MHz,  $\text{CD}_2\text{Cl}_2$ , 298 K)  $\delta$  164.9 (s, OCN), 147.6 (s,  $\text{C}^{2,6}$   $\text{C}_5\text{H}_3\text{N}$ ), 133.0 (s,  $\text{C}^4$   $\text{C}_5\text{H}_3\text{N}$ ), 122.7 (s,  $\text{C}^{3,5}$   $\text{C}_5\text{H}_3\text{N}$ ), 73.6 (d,  $^3J_{\text{CP}} = 6$  Hz,  $\text{NCH}_2\text{N}$ ), 72.4 (s,  $\text{CH}^i\text{Pr}$ ), 71.1 (s,  $\text{OCH}_2$ ), 53.3 (d,  $J_{\text{CP}} = 12$  Hz,  $\text{NCH}_2\text{P}$ ), 29.0 (s,  $\text{CHMe}_2$ ), 19.1, 14.2 (2s,  $\text{CHMe}_2$ ) ppm.  $^{31}\text{P}\{^1\text{H}\}$  NMR (161.95 MHz,  $\text{CD}_2\text{Cl}_2$ , 298 K)  $\delta$  –41.5 (s) ppm.

**1c** Yield: 0.397 g, 90%.  $S_{293\text{ K}}$  ( $\text{H}_2\text{O}$ ): 31.40 mg/mL.  $^1\text{H}$  NMR (300.13 MHz,  $\text{CD}_2\text{Cl}_2$ , 298 K)  $\delta$  7.81 (m, 3H,  $\text{H}^{3,4,5}$   $\text{C}_5\text{H}_3\text{N}$ ), 4.85–4.69 (m, 10H,  $\text{OCH}_2$ ,  $\text{NCH}_2\text{N}$ ), 4.56 (m, 6H,  $\text{NCH}_2\text{P}$ ), 3.97 (m, 2H,  $\text{CH}^i\text{Pr}$ ), 2.27 (m, 2H,  $\text{CHMe}_2$ ), 1.07 (d,  $^3J_{\text{HH}} = 7.6$  Hz, 6H,  $\text{CHMe}_2$ ), 0.72 (d,  $^3J_{\text{HH}} = 6.4$  Hz, 6H,  $\text{CHMe}_2$ ) ppm.  $^{13}\text{C}\{^1\text{H}\}$  NMR (100.61 MHz,  $\text{CD}_2\text{Cl}_2$ , 298 K)  $\delta$  164.9 (s, OCN), 147.6 (s,  $\text{C}^{2,6}$   $\text{C}_5\text{H}_3\text{N}$ ), 133.0 (s,  $\text{C}^4$   $\text{C}_5\text{H}_3\text{N}$ ), 122.7 (s,  $\text{C}^{3,5}$   $\text{C}_5\text{H}_3\text{N}$ ), 73.6 (d,  $^3J_{\text{CP}} = 6$  Hz,  $\text{NCH}_2\text{N}$ ), 72.4 (s,  $\text{CH}^i\text{Pr}$ ), 71.1 (s,  $\text{OCH}_2$ ), 53.3 (d,  $J_{\text{CP}} = 12$  Hz,  $\text{NCH}_2\text{P}$ ), 29.0 (s,  $\text{CHMe}_2$ ), 19.1, 14.2 (2s,  $\text{CHMe}_2$ ) ppm.  $^{31}\text{P}\{^1\text{H}\}$  NMR (161.95 MHz,  $\text{CD}_2\text{Cl}_2$ , 298 K)  $\delta$  –41.0 (s) ppm.

**Synthesis of complexes *trans*-[RuCl<sub>2</sub>{(*R,R*)-Ph-pybox}(1-H-PTA)][Cl] (2a), *trans*-[RuCl<sub>2</sub>{(*S,S*)-*i*Pr-pybox}(1-H-PTA)][Cl] (2b) and *trans*-[RuCl<sub>2</sub>{(*R,R*)-*i*Pr-pybox}(1-H-PTA)][Cl] (2c).** To a solution of 0.13 mmol of the corresponding complex *trans*-[RuCl<sub>2</sub>{(*R,R*)-Ph-pybox}(PTA)] (1a), *trans*-[RuCl<sub>2</sub>{(*S,S*)-*i*Pr-pybox}(PTA)] (1b) or *trans*-[RuCl<sub>2</sub>{(*R,R*)-*i*Pr-pybox}(PTA)] (1c) in dichloromethane (3 mL) at –30 °C, an equimolar amount of HCl (2M diethyl ether solution) was added and the resulting mixture was stirred for 2 hours. The addition of hexane (25 mL) afforded a dark pink solid precipitate. Solvents were decanted and the solid residue was washed with hexane (2 x 10 mL) and dried under vacuum.

**2a** Yield: 0.076 g, 80%. Conductivity (acetone, 293 K):  $\Lambda = 12\text{ S cm}^2\text{ mol}^{-1}$ .  $S_{293\text{ K}}$  ( $\text{H}_2\text{O}$ ): 9.70 mg/mL. Anal. Calcd. for  $\text{C}_{29}\text{H}_{32}\text{Cl}_3\text{N}_6\text{O}_2\text{PRu}\cdot\text{ICH}_2\text{Cl}_2$ : C, 43.94; H, 4.18; N, 10.25. Found: C, 43.67; H, 4.85; N, 10.56.  $^1\text{H}$  NMR (400.13 MHz,  $\text{CD}_2\text{Cl}_2$ , 298 K)  $\delta$  8.09 (m, 3H,  $\text{H}^{3,4,5}$   $\text{C}_5\text{H}_3\text{N}$ ), 7.55–7.30 (m, 10H, Ph), 5.25 (m, 2H,  $\text{OCH}_2$ ), 5.14 (m, 2H,  $\text{CHPh}$ ), 4.56 (m, 6H,  $\text{OCH}_2$ ,  $\text{NCH}_2\text{N}$ , NH), 4.18 (m, 3H,  $\text{NCH}_2\text{N}$ ), 3.60 (m, 3H,  $\text{NCH}_2\text{P}$ ), 3.46 (m, 3H,  $\text{NCH}_2\text{P}$ ) ppm.  $^{13}\text{C}\{^1\text{H}\}$  NMR (100.61 MHz,  $\text{CD}_2\text{Cl}_2$ , 298 K)  $\delta$  167.2 (s, OCN), 147.7 (s,  $\text{C}^{2,6}$   $\text{C}_5\text{H}_3\text{N}$ ), 138.8 (s,  $\text{C}^{ipso}$  Ph), 134.9 (s,  $\text{C}^4$   $\text{C}_5\text{H}_3\text{N}$ ), 129.3, 129.1, 127.9 (3s, Ph), 124.3 (s,  $\text{C}^{3,5}$   $\text{C}_5\text{H}_3\text{N}$ ), 78.9 (s,  $\text{OCH}_2$ ), 71.4 (s,  $\text{NCH}_2\text{N}$ ), 70.8 (s,  $\text{CHPh}$ ), 49.9 (br,  $\text{NCH}_2\text{P}$ ) ppm.  $^{31}\text{P}\{^1\text{H}\}$  NMR (162.1 MHz,  $\text{CD}_2\text{Cl}_2$ , 298 K)  $\delta$  –27.9 (s) ppm.

**2b** Yield: 0.075 g, 86%. Conductivity (acetone, 293 K):  $\Lambda = 17\text{ S cm}^2\text{ mol}^{-1}$ .  $S_{293\text{ K}}$  ( $\text{H}_2\text{O}$ ): 22.45 mg/mL. MS-ESI (MeOH):  $m/z = 631.0$   $[\text{RuCl}_2(\text{Pr-pybox})(1\text{-H-PTA})]^+$  (98 %), 595.0  $[\text{RuCl}(\text{Pr-pybox})(1\text{-H-PTA})]^+$  (55 %).  $^1\text{H}$  NMR (400.13 MHz,  $\text{CD}_2\text{Cl}_2$ , 298 K)  $\delta$  7.96 (m, 1H,  $\text{H}^4$   $\text{C}_5\text{H}_3\text{N}$ ), 7.87 (m, 2H,  $\text{H}^{3,5}$   $\text{C}_5\text{H}_3\text{N}$ ), 4.99 (br, 6H,  $\text{NCH}_2\text{N}$ , NH), 4.83 (m, 3H,  $\text{OCH}_2$ ,  $\text{NCH}_2\text{N}$ ), 4.72 (m, 2H,  $\text{OCH}_2$ ), 4.60 (br, 6H,  $\text{NCH}_2\text{P}$ ), 4.01 (m, 2H,  $\text{CH}^i\text{Pr}$ ), 2.10 (m, 2H,  $\text{CHMe}_2$ ), 1.08 (d,  $^3J_{\text{HH}} = 6.8$  Hz, 6H,  $\text{CHMe}_2$ ), 0.72 (d,  $^3J_{\text{HH}} = 6.0$  Hz, 6H,  $\text{CHMe}_2$ ) ppm.  $^{13}\text{C}\{^1\text{H}\}$  NMR (100.61 MHz,  $\text{CD}_2\text{Cl}_2$ , 298 K)  $\delta$  164.8 (s, OCN), 147.4 (s,  $\text{C}^{2,6}$   $\text{C}_5\text{H}_3\text{N}$ ), 134.7 (s,  $\text{C}^4$   $\text{C}_5\text{H}_3\text{N}$ ), 123.1 (s,  $\text{C}^{3,5}$   $\text{C}_5\text{H}_3\text{N}$ ), 72.2 (s,  $\text{CH}^i\text{Pr}$ ), 72.1 (s,  $\text{NCH}_2\text{N}$ ), 71.3 (s,  $\text{OCH}_2$ ), 53.4 (s,  $\text{NCH}_2\text{P}$ ), 29.2 (s,  $\text{CHMe}_2$ ), 18.9, 14.1 (2s,  $\text{CHMe}_2$ ) ppm.  $^{31}\text{P}\{^1\text{H}\}$  NMR (161.95 MHz,  $\text{CD}_2\text{Cl}_2$ , 298 K)  $\delta$  –24.9 (s) ppm.

**Synthesis of complexes *trans*-[RuCl<sub>2</sub>{(*R,R*)-Ph-pybox}(1-CH<sub>3</sub>-PTA)][I] (3a), *trans*-[RuCl<sub>2</sub>{(*S,S*)-*i*Pr-pybox}(1-CH<sub>3</sub>-PTA)][I] (3b), *trans*-[RuCl<sub>2</sub>{(*R,R*)-*i*Pr-pybox}(1-CH<sub>3</sub>-PTA)][I] (3c).** To a solution of 0.13 mmol of the corresponding complex 1a, 1b or 1c in dichloromethane (3 mL), an excess of the methyl iodide (40  $\mu\text{L}$ , 0.65 mmol) was added and the resulting mixture was stirred at room temperature for 2 hours. The addition of diethyl ether (50 mL) (3a) or hexane (40 mL) (3b, 3c) afforded a dark pink solid precipitate. Solvents were decanted and the solid residue was washed with diethyl ether (3a) or hexane (3b, 3c) (2 x 10 mL) and dried under vacuum.

**3a** Yield: 0.088 g, 81%. Conductivity (acetone, 293 K):  $\Lambda = 90\text{ S cm}^2\text{ mol}^{-1}$ .  $S_{293\text{ K}}$  ( $\text{H}_2\text{O}$ ): 5.54 mg/mL. Anal. Calcd. for  $\text{C}_{30}\text{H}_{34}\text{Cl}_2\text{IN}_6\text{O}_2\text{PRu}\cdot\text{ICH}_2\text{Cl}_2$ : C, 40.23; H, 3.92; N, 9.08. Found: C, 40.50; H, 4.12; N, 9.14.  $^1\text{H}$  NMR (300.13 MHz,  $\text{CD}_2\text{Cl}_2$ , 298 K)  $\delta$  8.11 (m, 3H,  $\text{H}^{3,4,5}$   $\text{C}_5\text{H}_3\text{N}$ ), 7.47 (m, 10H, Ph), 5.53 (m, 2H,  $\text{R-NCH}_2\text{N}$ ), 5.30 (m, 4H,  $\text{OCH}_2$ ,  $\text{CHPh}$ ), 4.57 (m, 5H,  $\text{OCH}_2$ ,  $\text{NCH}_2\text{N}$ ,  $\text{R-NCH}_2\text{N}$ ), 3.77 (m, 4H,  $\text{NCH}_2\text{N}$ ,  $\text{R-NCH}_2\text{P}$ ,  $\text{NCH}_2\text{P}$ ), 3.49 (m, 2H,  $\text{NCH}_2\text{P}$ ), 3.26 (m, 1H,  $\text{NCH}_2\text{P}$ ), 2.65 (s, 3H,  $\text{NCH}_3$ ) ppm.  $^{13}\text{C}\{^1\text{H}\}$  NMR (75.48 MHz,  $\text{CD}_2\text{Cl}_2$ , 298 K)  $\delta$  167.2 (s, OCN), 147.6 (s,  $\text{C}^{2,6}$   $\text{C}_5\text{H}_3\text{N}$ ), 139.1 (s,  $\text{C}^{ipso}$  Ph), 135.4 (s,  $\text{C}^4$   $\text{C}_5\text{H}_3\text{N}$ ), 129.3, 128.9, 128.2 (3s, Ph), 124.4 (s,  $\text{C}^{3,5}$   $\text{C}_5\text{H}_3\text{N}$ ), 80.5 (d,  $^3J_{\text{CP}} = 3$  Hz,  $\text{R-NCH}_2\text{N}$ ), 80.4 (d,  $^3J_{\text{CP}} = 3$  Hz,  $\text{R-NCH}_2\text{N}$ ), 78.9 (s,  $\text{OCH}_2$ ), 70.6 (s,  $\text{CHPh}$ ), 69.4 (d,  $^3J_{\text{CP}} = 5$  Hz,  $\text{NCH}_2\text{N}$ ), 59.3 (d,  $J_{\text{CP}} = 7$  Hz,  $\text{R-NCH}_2\text{P}$ ), 49.3 (s,  $\text{NCH}_3$ ), 49.1 (d,  $J_{\text{CP}} = 16$  Hz,  $\text{NCH}_2\text{P}$ ), 48.7 (d,  $J_{\text{CP}} = 16$  Hz,  $\text{NCH}_2\text{P}$ ) ppm.  $^{31}\text{P}\{^1\text{H}\}$  NMR (121.49 MHz,  $\text{CD}_2\text{Cl}_2$ , 298 K)  $\delta$  –18.4 (br) ppm.

**3b** Yield: 0.077 g, 77%. Conductivity (acetone, 293 K):  $\Lambda = 98\text{ S cm}^2\text{ mol}^{-1}$ .  $S_{293\text{ K}}$  ( $\text{H}_2\text{O}$ ): 7.10 mg/mL. Anal. Calcd. for  $\text{C}_{24}\text{H}_{38}\text{Cl}_2\text{IN}_6\text{O}_2\text{PRu}\cdot\text{1/2CH}_2\text{Cl}_2$ : C, 36.11; H, 4.82; N, 10.31. Found: C, 36.35; H, 5.17; N, 10.22.  $^1\text{H}$  NMR (400.13 MHz,  $\text{CD}_2\text{Cl}_2$ , 298 K)  $\delta$  7.98 (m, 1H,  $\text{H}^4$   $\text{C}_5\text{H}_3\text{N}$ ), 7.89 (m, 2H,  $\text{H}^{3,5}$   $\text{C}_5\text{H}_3\text{N}$ ), 5.69 (m, 2H,  $\text{NCH}_2\text{N}$ ), 5.47 (m, 2H,  $\text{NCH}_2\text{N}$ ), 4.96 (m, 2H,  $\text{NCH}_2\text{N}$ ), 4.85 (m, 2H,  $\text{OCH}_2$ ), 4.74 (pt, 2H,  $^3J_{\text{HH}} = 9.4$  Hz,  $^2J_{\text{HH}} = 9.4$  Hz,  $\text{OCH}_2$ ), 4.49



(m, 6H, NCH<sub>2</sub>P), 4.20 (m, 2H, CH<sup>β</sup>Pr), 3.29 (s, 3H, NCH<sub>3</sub>), 2.06 (m, 2H, CHMe<sub>2</sub>), 1.10 (d, <sup>3</sup>J<sub>HH</sub> = 7.2 Hz, 6H, CHMe<sub>2</sub>), 0.71 (d, <sup>3</sup>J<sub>HH</sub> = 6.8 Hz, 6H, CHMe<sub>2</sub>) ppm. <sup>31</sup>P{<sup>1</sup>H} NMR (161.95 MHz, CD<sub>2</sub>Cl<sub>2</sub>, 298 K) δ -16.0 (s) ppm.

**Synthesis of complexes *trans*-[RuCl<sub>2</sub>{(*R,R*)-Ph-pybox}(1-CH<sub>2</sub>=CHCH<sub>2</sub>-PTA)][I] (4a), *trans*-[RuCl<sub>2</sub>{(*S,S*)-<sup>i</sup>Pr-pybox}(1-CH<sub>2</sub>=CHCH<sub>2</sub>-PTA)][I] (4b) and *trans*-[RuCl<sub>2</sub>{(*R,R*)-<sup>i</sup>Pr-pybox}(1-CH<sub>2</sub>=CHCH<sub>2</sub>-PTA)][I] (4c)** To a solution of 0.13 mmol of the corresponding complex **1a**, **1b** or **1c** in dichloromethane (3 mL), the allyl iodide (24 μL, 0.26 mmol (for **1a**) or 12 μL, 0.13 mmol (for **1b**, **1c**)) was added, and the resulting mixture was stirred at room temperature for 2 hours. The addition of diethyl ether (40 mL) (**4a**) or hexane (30 mL) (**4b**, **4c**) afforded a dark pink solid precipitate. Solvents were decanted and the solid residue was washed with diethyl ether (**4a**) or hexane (**4b**, **4c**) (2 x 10 mL) and dried under vacuum.

**4a** Yield: 0.101 g, 90%. Conductivity (acetone, 293 K):  $\Lambda = 90 \text{ S cm}^2 \text{ mol}^{-1}$ . S<sub>293 K</sub> (H<sub>2</sub>O): 2.45 mg/mL. Anal. Calcd. for C<sub>32</sub>H<sub>36</sub>Cl<sub>2</sub>IN<sub>6</sub>O<sub>2</sub>PRu: C, 44.36; H, 4.19; N, 9.70. Found: C, 42.94; H, 4.10; N, 9.25. <sup>1</sup>H NMR (300.13 MHz, CD<sub>2</sub>Cl<sub>2</sub>, 298 K) δ 8.12 (br, 3H, H<sup>3,4,5</sup> C<sub>5</sub>H<sub>3</sub>N), 7.45 (m, 10H, Ph), 5.76 (m, 2H, CH<sub>2</sub>=CHCH<sub>2</sub>), 5.57 (m, 2H, CH<sub>2</sub>=CHCH<sub>2</sub>), R-NCH<sub>2</sub>N), 5.29 (m, 4H, OCH<sub>2</sub>, CHPh), 4.63–4.45 (m, 5H, OCH<sub>2</sub>, R-NCH<sub>2</sub>N), 3.98–3.84 (m, 3H, NCH<sub>2</sub>N, R-NCH<sub>2</sub>P), 3.73–3.27 (m, 6H, CH<sub>2</sub>=CHCH<sub>2</sub>, R-NCH<sub>2</sub>P, NCH<sub>2</sub>P), 3.24 (m, 1H, NCH<sub>2</sub>P) ppm. <sup>13</sup>C{<sup>1</sup>H} NMR (75.48 MHz, CD<sub>2</sub>Cl<sub>2</sub>, 298 K) δ 167.2 (s, OCN), 147.5 (s, C<sup>2,6</sup> C<sub>5</sub>H<sub>3</sub>N), 139.1 (s, C<sup>ipso</sup> Ph), 135.3 (s, C<sup>4</sup> C<sub>5</sub>H<sub>3</sub>N), 129.9 (s, CH<sub>2</sub>=CHCH<sub>2</sub>), 129.2, 128.8, 128.0 (3s, Ph), 124.3 (s, C<sup>3,5</sup> C<sub>5</sub>H<sub>3</sub>N), 122.2 (s, CH<sub>2</sub>=CHCH<sub>2</sub>), 79.3 (s, R-NCH<sub>2</sub>N), 79.0 (s, OCH<sub>2</sub>), 78.5 (s, R-NCH<sub>2</sub>N), 70.5 (s, CHPh), 69.6 (s, NCH<sub>2</sub>N), 63.2 (s, CH<sub>2</sub>=CHCH<sub>2</sub>), 55.6 (s, R-NCH<sub>2</sub>P), 49.7, 49.4 (2br s, NCH<sub>2</sub>P) ppm. <sup>31</sup>P{<sup>1</sup>H} NMR (121.49 MHz, CD<sub>2</sub>Cl<sub>2</sub>, 298 K) δ -15.2 (s) ppm.

**4b** Yield: 0.073 g, 70%. Conductivity (acetone, 293 K):  $\Lambda = 91 \text{ S cm}^2 \text{ mol}^{-1}$ . S<sub>293 K</sub> (H<sub>2</sub>O): 9.16 mg/mL. Anal. Calcd. for C<sub>26</sub>H<sub>40</sub>Cl<sub>2</sub>IN<sub>6</sub>O<sub>2</sub>PRu·1/2CH<sub>2</sub>Cl<sub>2</sub>: C, 37.85; H, 4.91; N, 9.99. Found: C, 37.56; H, 4.59; N, 10.59. <sup>1</sup>H NMR (400.13 MHz, CD<sub>2</sub>Cl<sub>2</sub>, 298 K) δ 7.97 (m, 1H, H<sup>4</sup> C<sub>5</sub>H<sub>3</sub>N), 7.87 (m, 2H, H<sup>3,5</sup> C<sub>5</sub>H<sub>3</sub>N), 6.09 (m, 1H, CH<sub>2</sub>=CHCH<sub>2</sub>), 5.97–5.83 (m, 3H, CH<sub>2</sub>=CHCH<sub>2</sub>, R-NCH<sub>2</sub>N), 5.47 (m, 1H, R-NCH<sub>2</sub>N), 5.25 (m, 1H, R-NCH<sub>2</sub>N), 5.04 (m, 1H, NCH<sub>2</sub>N), 4.93 (m, 1H, R-NCH<sub>2</sub>P), 4.82–4.72 (m, 6H, OCH<sub>2</sub>, R-NCH<sub>2</sub>P), 4.55–4.35 (m, 7H, NCH<sub>2</sub>N, NCH<sub>2</sub>P, CH<sub>2</sub>=CHCH<sub>2</sub>), 4.17 (m, 2H, CH<sup>β</sup>Pr), 2.05 (m, 2H, CHMe<sub>2</sub>), 1.09 (d, <sup>3</sup>J<sub>HH</sub> = 6.4 Hz, 6H, CHMe<sub>2</sub>), 0.70 (d, <sup>3</sup>J<sub>HH</sub> = 5.2 Hz, 6H, CHMe<sub>2</sub>) ppm. <sup>13</sup>C{<sup>1</sup>H} NMR (100.61 MHz, CD<sub>2</sub>Cl<sub>2</sub>, 298 K) δ 164.8 (s, OCN), 147.4 (s, C<sup>2,6</sup> C<sub>5</sub>H<sub>3</sub>N), 135.3 (s, C<sup>4</sup> C<sub>5</sub>H<sub>3</sub>N), 130.5 (s, CH<sub>2</sub>=CHCH<sub>2</sub>), 123.3 (s, C<sup>3,5</sup> C<sub>5</sub>H<sub>3</sub>N), 122.8 (CH<sub>2</sub>=CHCH<sub>2</sub>), 79.6, 79.2 (2s, R-NCH<sub>2</sub>N), 73.3 (d, <sup>3</sup>J<sub>CP</sub> = 5 Hz, NCH<sub>2</sub>N), 72.0 (s, CH<sup>β</sup>Pr), 71.5 (s, OCH<sub>2</sub>), 70.4 (s, NCH<sub>2</sub>N), 63.4 (s, CH<sub>2</sub>=CHCH<sub>2</sub>), 55.5 (d, <sup>3</sup>J<sub>CP</sub> = 16 Hz, R-NCH<sub>2</sub>P), 50.6 (d, <sup>3</sup>J<sub>CP</sub> = 16 Hz, NCH<sub>2</sub>P), 50.4 (d, <sup>3</sup>J<sub>CP</sub> = 14 Hz, NCH<sub>2</sub>P), 29.4 (s, CHMe<sub>2</sub>), 19.0, 14.3 (2s, CHMe<sub>2</sub>) ppm. <sup>31</sup>P{<sup>1</sup>H} NMR (161.95 MHz, CD<sub>2</sub>Cl<sub>2</sub>, 298 K) δ -14.2 (s) ppm.

**Synthesis of complexes *trans*-[RuCl<sub>2</sub>{(*R,R*)-Ph-pybox}(1-CH≡CCH<sub>2</sub>-PTA)][Br] (5a), *trans*-[RuCl<sub>2</sub>{(*S,S*)-<sup>i</sup>Pr-pybox}(1-CH≡CCH<sub>2</sub>-PTA)][Br] (5b) and *trans*-[RuCl<sub>2</sub>{(*R,R*)-<sup>i</sup>Pr-pybox}(1-CH≡CCH<sub>2</sub>-PTA)][Br] (5c)** To a solution of 0.13 mmol of the corresponding complex **1a**, **1b** or **1c** in dichloromethane (5 mL), an excess of the propargyl bromide was added (58 μL, 0.650 mmol), and the resulting mixture was stirred at room temperature for 2 hours. The addition of diethyl ether (40 mL) (**5a**) of hexane (40 mL) (**5b**, **5c**) afforded a dark pink solid precipitate. Solvents were decanted and the solid residue was washed with diethyl ether (**5a**) or hexane (**5b**, **5c**) (2 x 10 mL) and dried under vacuum.

**5a** Yield: 0.103 g, 97%. Conductivity (acetone, 293 K):  $\Lambda = 97 \text{ S cm}^2 \text{ mol}^{-1}$ . S<sub>293 K</sub> (H<sub>2</sub>O): 6.90 mg/mL. Anal. Calcd. for C<sub>32</sub>H<sub>34</sub>BrCl<sub>2</sub>N<sub>6</sub>O<sub>2</sub>PRu·1CH<sub>2</sub>Cl<sub>2</sub>: C, 43.92; H, 4.02; N, 9.31. Found: C, 43.18; H, 4.48; N, 9.51. <sup>1</sup>H NMR (300.13 MHz, CD<sub>2</sub>Cl<sub>2</sub>, 298 K) δ 8.11 (m, 3H, H<sup>3,4,5</sup> C<sub>5</sub>H<sub>3</sub>N), 7.47 (m, 10H, Ph), 5.71 (m, 2H, R-NCH<sub>2</sub>N), 5.33–5.23 (m, 5H, OCH<sub>2</sub>, CHPh, CH≡CCH<sub>2</sub>), 4.87 (m, 1H, R-NCH<sub>2</sub>N), 4.70 (m, 1H, R-NCH<sub>2</sub>N), 4.59 (m, 3H, OCH<sub>2</sub>, NCH<sub>2</sub>N), 4.46 (m, 1H, R-NCH<sub>2</sub>P), 4.00–3.43 (m, 6H, NCH<sub>2</sub>P, NCH<sub>2</sub>N, R-NCH<sub>2</sub>P, CH≡CCH<sub>2</sub>), 3.38 (m, 2H, NCH<sub>2</sub>P) ppm. <sup>13</sup>C{<sup>1</sup>H} NMR (100.61 MHz, CD<sub>2</sub>Cl<sub>2</sub>, 298 K) δ 167.2 (s, OCN), 147.6 (s, C<sup>2,6</sup> C<sub>5</sub>H<sub>3</sub>N), 138.9 (s, C<sup>ipso</sup> Ph), 135.3 (s, C<sup>4</sup> C<sub>5</sub>H<sub>3</sub>N), 129.2, 128.9, 128.2 (3s, Ph), 124.3 (s, C<sup>3,5</sup> C<sub>5</sub>H<sub>3</sub>N), 81.8 (s, CH<sub>2</sub>C≡CH), 79.4 (s, R-NCH<sub>2</sub>N), 79.1 (s, OCH<sub>2</sub>), 78.9 (s, R-NCH<sub>2</sub>N), 70.5 (s, CH≡CCH<sub>2</sub>, CHPh (overlapped signals)), 69.6 (s, NCH<sub>2</sub>N), 55.9 (s, CH≡CCH<sub>2</sub>), 51.1 (s, R-NCH<sub>2</sub>P), 49.2, 49.1 (2br s, NCH<sub>2</sub>P) ppm. <sup>31</sup>P{<sup>1</sup>H} NMR (121.49 MHz, CD<sub>2</sub>Cl<sub>2</sub>, 298 K) δ -15.7 (s) ppm.

**5b** Yield: 0.077 g, 79%. Conductivity (acetone, 293 K):  $\Lambda = 72 \text{ S cm}^2 \text{ mol}^{-1}$ . S<sub>293 K</sub> (H<sub>2</sub>O): 8.40 mg/mL. Anal. Calcd. for C<sub>26</sub>H<sub>38</sub>BrCl<sub>2</sub>N<sub>6</sub>O<sub>2</sub>PRu·1CH<sub>2</sub>Cl<sub>2</sub>: C, 38.86; H, 4.83; N, 10.07. Found: C, 38.70; H, 4.79; N, 10.44. <sup>1</sup>H NMR (400.13 MHz, CD<sub>2</sub>Cl<sub>2</sub>, 298 K) δ 7.98 (m, 1H, H<sup>4</sup> C<sub>5</sub>H<sub>3</sub>N), 7.90 (m, 2H, H<sup>3,5</sup> C<sub>5</sub>H<sub>3</sub>N), 5.96 (m, 2H, R-NCH<sub>2</sub>N), 5.71 (m, 1H, R-NCH<sub>2</sub>N), 5.50 (m, 1H, R-NCH<sub>2</sub>N), 5.26 (m, 1H, CH≡CCH<sub>2</sub>), 4.97–4.33 (m, 14H, CH≡CCH<sub>2</sub>, NCH<sub>2</sub>N, NCH<sub>2</sub>P, OCH<sub>2</sub>, CH≡CCH<sub>2</sub>), 4.22 (m, 2H, CH<sup>β</sup>Pr), 2.08 (m, 2H, CHMe<sub>2</sub>), 1.10 (d, <sup>3</sup>J<sub>HH</sub> = 6.8 Hz, 6H, CHMe<sub>2</sub>), 0.72 (d, <sup>3</sup>J<sub>HH</sub> = 6.4 Hz, 6H, CHMe<sub>2</sub>) ppm. <sup>13</sup>C{<sup>1</sup>H} NMR (100.61 MHz, CD<sub>2</sub>Cl<sub>2</sub>, 298 K) δ 164.7 (s, OCN), 147.4 (s, C<sup>2,6</sup> C<sub>5</sub>H<sub>3</sub>N), 135.3 (s, C<sup>4</sup> C<sub>5</sub>H<sub>3</sub>N), 123.4 (s, C<sup>3,5</sup> C<sub>5</sub>H<sub>3</sub>N), 81.9 (s, CH≡CCH<sub>2</sub>), 79.7, 79.4 (2s, R-NCH<sub>2</sub>N), 71.9 (s, CH<sup>β</sup>Pr), 71.5 (s, OCH<sub>2</sub>), 70.4 (s, NCH<sub>2</sub>N), 70.1 (s, CH≡CCH<sub>2</sub>), 55.7 (s, CH≡CCH<sub>2</sub>), 51.2 (s, R-NCH<sub>2</sub>P), 50.4 (d, <sup>3</sup>J<sub>CP</sub> = 16 Hz, NCH<sub>2</sub>P), 50.2 (d, <sup>3</sup>J<sub>CP</sub> = 14 Hz, NCH<sub>2</sub>P), 29.4 (s, CHMe<sub>2</sub>), 19.0, 14.3 (s, CHMe<sub>2</sub>) ppm. <sup>31</sup>P{<sup>1</sup>H} NMR (161.95 MHz, CD<sub>2</sub>Cl<sub>2</sub>, 298 K) δ -13.7 (s) ppm.

**Synthesis of complexes *trans*-[RuCl<sub>2</sub>{(*R,R*)-Ph-pybox}(1-PhCH<sub>2</sub>-PTA)][Br] (6a), *trans*-[RuCl<sub>2</sub>{(*S,S*)-<sup>i</sup>Pr-pybox}(1-PhCH<sub>2</sub>-PTA)][Br] (6b), *trans*-[RuCl<sub>2</sub>{(*R,R*)-<sup>i</sup>Pr-pybox}(1-PhCH<sub>2</sub>-PTA)][Br] (6c), *trans*-[RuCl<sub>2</sub>{(*R,R*)-Ph-pybox}(1-PhCH<sub>2</sub>-PTA)][Cl] (7a) and *trans*-[RuCl<sub>2</sub>{(*R,R*)-<sup>i</sup>Pr-pybox}(1-PhCH<sub>2</sub>-PTA)][Cl] (7c)** To a solution of 0.13 mmol of the corresponding complex **1a**, **1b** or **1c** in dichloromethane (5 mL), an excess of the benzyl bromide or benzyl chloride (0.650 mmol, 77 μL (**6b**, **6c**), 75 μL (**7c**) or 1.30 mmol, 154 μL (**6a**), 150 μL (**7a**)) was added and

the resulting mixture was stirred at room temperature. The addition of diethyl ether (40 mL) (**6a**, **7a**) or hexane (20 mL) (**6b**, **6c**, **7c**) afforded a dark pink solid precipitate. Solvents were decanted and the solid residue was washed with diethyl ether (**6a**, **7a**) or hexane (**6b**, **6c**, **7c**) (2 x 10 mL) and dried under vacuum.

**6a** Yield: 0.079 g, 70%. Reaction time: 2 h. Conductivity (acetone, 293 K):  $\Lambda = 82 \text{ S cm}^2 \text{ mol}^{-1}$ .  $S_{293 \text{ K}}(\text{H}_2\text{O})$ : 4.89 mg/mL. MS-ESI (MeOH):  $m/z = 789.0$   $[\text{RuCl}_2(\text{Ph-pybox})(1\text{-PhCH}_2\text{-PTA})]^+$  (100%).  $^1\text{H-NMR}$  (300.13 MHz,  $\text{CD}_2\text{Cl}_2$ , 298 K)  $\delta$  8.09 (m, 3H,  $\text{H}^{3,4,5} \text{ C}_5\text{H}_3\text{N}$ ), 7.61–7.25 (3m, 15H, Ph,  $\text{CH}_2\text{Ph}$ ), 5.95 (m, 1H, R- $\text{NCH}_2\text{N}$ ), 5.79 (m, 1H, R- $\text{NCH}_2\text{N}$ ), 5.21 (m, 5H,  $\text{OCH}_2$ ,  $\text{CH}_2\text{Ph}$ ,  $\text{CHPh}$ ), 4.55 (m, 3H,  $\text{OCH}_2$ ,  $\text{NCH}_2\text{N}$ ), 4.43 (m, 1H, R- $\text{NCH}_2\text{P}$ ), 4.22 (m, 2H, R- $\text{NCH}_2\text{N}$ ), 3.98 (m, 1H,  $\text{NCH}_2\text{N}$ ), 3.83 (m, 1H,  $\text{NCH}_2\text{P}$ ), 3.60 (m, 2H, R- $\text{NCH}_2\text{P}$ ,  $\text{CH}_2\text{Ph}$ ), 3.20 (m, 2H,  $\text{NCH}_2\text{P}$ ), 2.91 (m, 1H,  $\text{NCH}_2\text{P}$ ) ppm.  $^{13}\text{C}\{^1\text{H}\}$  NMR (100.61 MHz,  $\text{CD}_2\text{Cl}_2$ , 298 K)  $\delta$  167.2 (d,  $^4J_{\text{CP}} = 4 \text{ Hz}$ , OCN), 147.5 (s,  $\text{C}^{2,6} \text{ C}_5\text{H}_3\text{N}$ ), 139.0 (s,  $\text{C}^{\text{ipso}} \text{ Ph}$ ), 137.7 (s,  $\text{C}^{\text{ipso}} \text{ CH}_2\text{Ph}$ ), 135.3 (s,  $\text{C}^4 \text{ C}_5\text{H}_3\text{N}$ ), 133.3, 130.6, 129.3, 129.0, 128.7, 128.6, 128.4, 127.9, 125.6 (9s, Ph,  $\text{CH}_2\text{Ph}$ ), 124.3 (s,  $\text{C}^{3,5} \text{ C}_5\text{H}_3\text{N}$ ), 79.5 (s, R- $\text{NCH}_2\text{N}$ ), 79.1 (s,  $\text{OCH}_2$ ), 78.4 (s, R- $\text{NCH}_2\text{N}$ ), 70.5 (s,  $\text{CHPh}$ ), 69.6 (s,  $\text{NCH}_2\text{N}$ ), 64.8 (s,  $\text{CH}_2\text{Ph}$ ), 54.6 (d,  $J_{\text{CP}} = 7 \text{ Hz}$ , R- $\text{NCH}_2\text{P}$ ), 49.6 (d,  $J_{\text{CP}} = 14 \text{ Hz}$ ,  $\text{NCH}_2\text{P}$ ), 49.3 (d,  $J_{\text{CP}} = 13 \text{ Hz}$ ,  $\text{NCH}_2\text{P}$ ) ppm.  $^{31}\text{P}\{^1\text{H}\}$  NMR (121.49 MHz,  $\text{CD}_2\text{Cl}_2$ , 298 K)  $\delta$  –15.4 (s) ppm.

**6b** Yield: 0.092 g, 88%. Reaction time: 1.5 h. Conductivity (acetone, 293 K):  $\Lambda = 68 \text{ S cm}^2 \text{ mol}^{-1}$ .  $S_{293 \text{ K}}(\text{H}_2\text{O})$ : 11.49 mg/mL. Anal. Calcd. for  $\text{C}_{30}\text{H}_{42}\text{BrCl}_2\text{N}_6\text{O}_2\text{PRu}\cdot\text{ICH}_2\text{Cl}_2$ : C, 42.00; H, 5.00; N, 9.48. Found: C, 41.75; H, 5.39; N, 9.34.  $^1\text{H NMR}$  (400.13 MHz,  $\text{CD}_2\text{Cl}_2$ , 298 K)  $\delta$  7.97 (m, 1H,  $\text{H}^4 \text{ C}_5\text{H}_3\text{N}$ ), 7.87 (m, 2H,  $\text{H}^{3,5} \text{ C}_5\text{H}_3\text{N}$ ), 7.71–7.38 (m, 5H, Ph), 6.31 (m, 2H,  $\text{NCH}_2\text{N}$ ), 5.15 (m, 1H,  $\text{NCH}_2\text{N}$ ), 5.02 (m, 3H,  $\text{NCH}_2\text{N}$ ), 4.81 (m, 4H,  $\text{OCH}_2$ ,  $\text{NCH}_2\text{P}$ ), 4.71 (m, 3H,  $\text{OCH}_2$ ,  $\text{NCH}_2\text{P}$ ), 4.54 (m, 3H,  $\text{CH}_2\text{Ph}$ ,  $\text{NCH}_2\text{P}$ ), 4.36 (m, 1H,  $\text{NCH}_2\text{P}$ ), 4.12 (m, 1H,  $\text{NCH}_2\text{P}$ ), 3.97 (m, 2H,  $\text{CH}^i\text{Pr}$ ), 1.88 (m, 2H,  $\text{CHMe}_2$ ), 0.89 (d, 6H,  $^3J_{\text{HH}} = 7.2 \text{ Hz}$ ,  $\text{CHMe}_2$ ), 0.65 (d,  $^3J_{\text{HH}} = 6.8 \text{ Hz}$ , 6H,  $\text{CHMe}_2$ ) ppm.  $^{13}\text{C}\{^1\text{H}\}$  NMR (100.61 MHz,  $\text{CD}_2\text{Cl}_2$ , 298 K)  $\delta$  164.8, (d,  $^4J_{\text{CP}} = 4.0 \text{ Hz}$ , OCN), 147.4 (s,  $\text{C}^{2,6} \text{ C}_5\text{H}_3\text{N}$ ), 135.3 (s,  $\text{C}^4 \text{ C}_5\text{H}_3\text{N}$ ), 133.2, 130.8, 129.5, 129.0, 128.7, 128.4 (6s, Ph), 125.4 (s,  $\text{C}^{\text{ipso}} \text{ Ph}$ ), 123.3 (s,  $\text{C}^{3,5} \text{ C}_5\text{H}_3\text{N}$ ), 79.5, 79.2 (2s, R- $\text{NCH}_2\text{N}$ ), 72.0 (s,  $\text{CH}^i\text{Pr}$ ), 71.3 (s,  $\text{OCH}_2$ ), 70.2 (s,  $\text{NCH}_2\text{N}$ ), 65.1 (s,  $\text{PhCH}_2$ ), 55.5 (d,  $J_{\text{CP}} = 5 \text{ Hz}$ , R- $\text{NCH}_2\text{P}$ ), 50.8 (d,  $J_{\text{CP}} = 13 \text{ Hz}$ ,  $\text{NCH}_2\text{P}$ ), 50.4 (d,  $J_{\text{CP}} = 14 \text{ Hz}$ ,  $\text{NCH}_2\text{P}$ ), 29.3 (s,  $\text{CHMe}_2$ ), 18.7, 14.2 (2s,  $\text{CHMe}_2$ ) ppm.  $^{31}\text{P}\{^1\text{H}\}$  NMR (161.95 MHz,  $\text{CD}_2\text{Cl}_2$ , 298 K)  $\delta$  –14.2 (s) ppm.

**7a** Yield: 0.064 g, 60%. Reaction time: 2.5 h. Conductivity (acetone, 293 K):  $\Lambda = 84 \text{ S cm}^2 \text{ mol}^{-1}$ .  $S_{293 \text{ K}}(\text{H}_2\text{O})$ : 5.12 mg/mL. Anal. Calcd. for  $\text{C}_{36}\text{H}_{38}\text{Cl}_3\text{N}_6\text{O}_2\text{PRu}\cdot\text{ICH}_2\text{Cl}_2$ : C, 48.83; H, 4.43; N, 9.23. Found: C, 49.00; H, 4.52; N, 9.03.  $^1\text{H NMR}$  (300.13 MHz,  $\text{CD}_2\text{Cl}_2$ , 298 K)  $\delta$  8.09 (m, 3H,  $\text{H}^{3,4,5} \text{ C}_5\text{H}_3\text{N}$ ), 7.60–7.25 (3m, 15H, Ph,  $\text{CH}_2\text{Ph}$ ), 5.94 (m, 1H, R- $\text{NCH}_2\text{N}$ ), 5.79 (m, 1H, R- $\text{NCH}_2\text{N}$ ), 5.21 (m, 5H,  $\text{OCH}_2$ ,  $\text{CH}_2\text{Ph}$ ,  $\text{CHPh}$ ), 4.59 (m, 3H,  $\text{NCH}_2\text{N}$ ,  $\text{OCH}_2$ ), 4.43 (m, 1H, R- $\text{NCH}_2\text{P}$ ), 4.22 (m, 2H, R- $\text{NCH}_2\text{N}$ ), 3.98 (m, 1H,  $\text{NCH}_2\text{N}$ ), 3.83 (m, 1H,  $\text{NCH}_2\text{P}$ ), 3.60 (m, 2H, R- $\text{NCH}_2\text{P}$ ,  $\text{CH}_2\text{Ph}$ ), 3.20 (m, 2H,  $\text{NCH}_2\text{P}$ ), 2.91 (m, 1H,  $\text{NCH}_2\text{P}$ ) ppm.  $^{13}\text{C}\{^1\text{H}\}$  NMR (100.61 MHz,  $\text{CD}_2\text{Cl}_2$ , 298 K)  $\delta$  167.2 (d,  $^4J_{\text{CP}} = 4 \text{ Hz}$ , OCN), 147.7 (s,  $\text{C}^{2,6} \text{ C}_5\text{H}_3\text{N}$ ), 139.0 (s,  $\text{C}^{\text{ipso}} \text{ Ph}$ ), 137.7 (s,  $\text{C}^{\text{ipso}} \text{ CH}_2\text{Ph}$ ), 135.3 (s,  $\text{C}^4 \text{ C}_5\text{H}_3\text{N}$ ), 133.3, 130.6, 129.3, 129.0, 128.7, 128.6, 128.4, 127.9, 125.6 (9s, Ph,  $\text{CH}_2\text{Ph}$ ), 124.3 (s,  $\text{C}^{3,5} \text{ C}_5\text{H}_3\text{N}$ ), 79.2 (s, R- $\text{NCH}_2\text{N}$ ), 79.1 (s,  $\text{OCH}_2$ ), 78.4 (s, R- $\text{NCH}_2\text{N}$ ), 70.5 (s,  $\text{CHPh}$ ), 69.6 (s,  $\text{NCH}_2\text{N}$ ), 64.9 (s,  $\text{CH}_2\text{Ph}$ ), 54.6 (d,  $J_{\text{CP}} = 7 \text{ Hz}$ , R- $\text{NCH}_2\text{P}$ ), 49.6 (d,  $J_{\text{CP}} = 14 \text{ Hz}$ ,  $\text{NCH}_2\text{P}$ ), 49.3 (d,  $J_{\text{CP}} = 13 \text{ Hz}$ ,  $\text{NCH}_2\text{P}$ ) ppm.  $^{31}\text{P}\{^1\text{H}\}$  NMR (121.49 MHz,  $\text{CD}_2\text{Cl}_2$ , 298 K)  $\delta$  –15.1 (s) ppm.

### Electrochemical Measurements

Cyclic voltammetry measurements (298 K) were performed with a three-electrode system, using a platinum disk, a platinum wire and a silver wire as working, counter and reference electrodes respectively. Current and voltage parameters were controlled by using a  $\mu$ -AUTOLAB Type III. In a typical experiment, complex was dissolved under a nitrogen atmosphere in recently distilled and deoxygenated dichloromethane ( $5 \times 10^{-4} \text{ M}$  in the complex and  $0.1 \text{ M}$  in the electrolyte  $[\text{Bu}_4\text{N}][\text{BF}_4]$ ). The scan rate was  $0.2 \text{ V}\cdot\text{s}^{-1}$ . All values are referenced to the  $[\text{Fe}(\eta^5\text{-C}_5\text{H}_5)_2]^{+/0}$  couple ( $E^\circ_{1/2} = 0.150\text{V}$ ).

### X-Ray Crystal Structure Determination of Complexes 1b, 2a and 3b.

Crystals suitable for X-ray diffraction analysis were obtained, from saturated solutions of the complexes **1b**, **2a** and **3b** in dichloromethane, by slow diffusion of diethyl ether (**1b** and **3b**) or hexane (**2a**). The most relevant crystal and refinement data can be found in the supplementary material as Table 2.

In all cases data collection was performed on a Oxford Diffraction Xcalibur Nova single crystal diffractometer, using Cu-K $\alpha$  radiation ( $\lambda = 1.5418 \text{ \AA}$ ). Images were collected at a 65 mm fixed crystal-detector distance, using the oscillation method, with  $1^\circ$  oscillation and (10 – 50), (10 – 60), and (5 – 85) s, respectively, variable exposure time per image. Data collection strategy was calculated with the program CrysAlis Pro CCD.<sup>26</sup> Data reduction and cell refinement was performed with the program CrysAlis Pro RED.<sup>26</sup> An empirical absorption correction was applied using the SCALE3 ABSPACK algorithm as implemented in the program CrysAlis Pro RED.<sup>26</sup>

The software package WINGX<sup>27</sup> was used for space group determination, structure solution and refinement. The structure for the complexes **1b** and **2a** were solved by Patterson interpretation and phase expansion using DIRDIF.<sup>28</sup> The structure for the complex **3b** was solved by direct methods using SIR92.<sup>29</sup>

Isotropic least-squares refinement on  $F^2$  using SHELXL97<sup>30</sup> was performed. During the final stages of the refinements, all the positional parameters and the anisotropic temperature factors of all the non-H atoms were refined. The H atoms were geometrically located and their coordinates were refined riding on their parent atoms (except H(1N) for **2a**, the coordinates of the H atom were found from different Fourier maps and included in a refinement with isotropic parameters). For **3b**, solvent molecules in the structure were highly disordered and were impossible to



refine using conventional discrete-atom models. To resolve this issue, the contribution of solvent electron density was removed by the SQUEEZE/PLATON.<sup>31</sup>

The function minimized was  $(\sum w(F_o^2 - F_c^2)/\sum w(F_o^2))^{1/2}$  where  $w = 1/[\sigma^2(F_o^2) + (aP)^2 + bP]$  (for **1b**,  $a = 0.0743$ ,  $b = 0.6797$ , for **2a**,  $a = 0.0612$ ,  $b = 1.8305$  and for **3b**,  $a = 0.0947$ ,  $b = 7.9303$ ) with  $\sigma(F_o^2)$  from counting statistics and  $P = (\text{Max}(F_o^2, 0) + 2F_c^2)/3$ .

Atomic scattering factors were taken from the International Tables for X-Ray Crystallography International.<sup>32</sup> Geometrical calculations were made with PARST.<sup>33</sup> The crystallographic plots were made with PLATON.<sup>31</sup>

CIF files for these complexes have been deposited in Cambridge Data Base<sup>34</sup>

#### DNA Mobility Shift Assays

Reactions between DNA and the ruthenium complexes were performed in a 10  $\mu$ L final volume in 10 mM sodium phosphate buffer at physiological pH 7.0, containing 0.5  $\mu$ g of the pBR322 plasmid (4361 base pairs, from Fermentas) and appropriate amounts of freshly prepared solution of the Ru complex also dissolved in phosphate buffer. Reaction mixtures were incubated for 14 hours at 37 °C. Ten microliters of the reactions were mixed with 1  $\mu$ L dye (0.025 mg bromophenol blue, 1mL glycerol and 1 mL distilled water) and they were analyzed by electrophoresis in 0.8% agarose gels in TBE buffer (Tris-Borate-EDTA). Gel running was conducted at a constant voltage of 3 V/cm. DNA bands were visualized by incubation of the gel with 1  $\mu$ g/mL ethidium bromide in TBE buffer for 10 minutes and photographed under UV light.

#### Cell cycle analysis.

For cell cycle analysis, we used the human cervical cancer HeLa cell line grown in DMEM supplemented with 10% (v/v) heat-inactivated fetal calf serum, 2 mM L-glutamine, 100 units/mL penicillin, and 100  $\mu$ g/mL streptomycin at 37 °C in a humidified atmosphere of 5% CO<sub>2</sub> and 95% air. Cells were periodically tested for *Mycoplasma* infection and found to be negative. Untreated and drug-treated cells ( $3\text{--}5 \times 10^5$ ) were centrifuged and fixed overnight in 70% ethanol at 4°C. Then, cells were washed three times with PBS, incubated for 1 h with 1 mg/mL RNase A and 20  $\mu$ g/mL propidium iodide at room temperature, and analyzed with a Becton Dickinson FACSCalibur flow cytometer (San Jose, CA) as described previously to determine the percentage of cells in each phase of the cell cycle.<sup>20,35</sup>

#### Conclusions

Overall, in this work we reported the synthesis of new water-soluble enantiopure ruthenium complexes *trans*-[RuCl<sub>2</sub>{(*S,S*)-Pr-pybox}(PTA)] (**1b**) and *trans*-[RuCl<sub>2</sub>{(*R,R*)-Pr-pybox}(PTA)] (**1c**), *trans*-[RuCl<sub>2</sub>{(*S,S*)-Pr-pybox}(1-H-PTA)][Cl] (**2b**) and *trans*-[RuCl<sub>2</sub>{(*R,R*)-Pr-pybox}(1-H-PTA)][Cl] (**2c**), and *trans*-[RuCl<sub>2</sub>{(*S,S*)-Pr-pybox}(1-R-PTA)][X] (**3b-6b**) and *trans*-[RuCl<sub>2</sub>{(*R,R*)-Pr-pybox}(1-R-PTA)][X] (**3c-6c**), containing the ligands 2,6-bis[4'(*S*)-isopropylloxazolin-2'-il-pyridine] ((*S,S*)-Pr-pybox) and 2,6-bis[4'(*R*)-isopropylloxazolin-2'-il-pyridine] ((*R,R*)-Pr-pybox) and water soluble 1,3,5-triaza-7-phosphaadamantane (PTA) or N-substituted PTA phosphanes. Analogous complexes (**1a-6a**) using 2,6-bis[4'(*R*)-phenyloxazolin-2'-il-pyridine] ((*R,R*)-Ph-pybox) have been also synthesized. The crystal X-ray structures of complexes **1b**, **3b** and **2a** are also reported.

The interactions with plasmidic DNA for the different enantiomers as well as its biological activity against microbes and as inducers of apoptosis in HeLa cells has been also analyzed. Despite the cytotoxic activity to HeLa cells of the ruthenium complexes was rather poor, requiring rather high drug concentrations and long incubation times to render DNA degradation, we found a different ability for ruthenium enantiomers to alter cell cycle, arresting cells at the G<sub>2</sub>/M phase, preceding cellular division, which eventually led to cell death after long incubation times. Thus, some ruthenium compounds bearing the (*R,R*)-Pr-pybox might behave as promoters of slow cell death in tumor cells. Further work will be necessary to analyze putative biomedical applications for these kinds of compounds.

**Acknowledgments.** Financial support came from Spanish MICINN (SAF2011-30518, CTQ2011-26481 and Consolider Ingenio 2010 (CSD2007-00006)). Red Temática de Investigación Cooperativa en Cáncer, Instituto de Salud Carlos III, cofunded by the Fondo Europeo de Desarrollo Regional of the European Union (RD06/0020/1037 and RD12/0036/0065), and Junta de Castilla y León (CSI052A11-2, CSI221A12-2). E. M. P. thanks the FICYT (Principado de Asturias) for a Ph.D. fellowship.

#### Notes and references

<sup>a</sup> Departamento de Química Orgánica e Inorgánica, Instituto de Química Organometálica "Enrique Moles" (Unidad Asociada al C.S.I.C.). Universidad de Oviedo, 33006 Oviedo, Principado de Asturias, Spain. E-mail: elb@uniovi.es (E. Lastra).

<sup>b</sup> Departamento de Biología Funcional, Instituto Universitario de Biotecnología de Asturias, Área de Microbiología. Universidad de Oviedo, 33006 Oviedo, Principado de Asturias, Spain.

<sup>c</sup> Instituto de Biología Molecular y Celular del Cáncer, Centro de Investigación del Cáncer, CSIC-Universidad de Salamanca, Campus Miguel de Unamuno, E-37007 Salamanca, Spain.

† Electronic Supplementary Information (ESI) available (32 pages): Experimental data for complexes **1c–7c**. Selected NMR spectra:  $^1\text{H}$ ,  $^{31}\text{P}\{^1\text{H}\}$ ,  $^{13}\text{C}\{^1\text{H}\}$ , DEPT 135 and selected bidimensional NMR experiments COSY HH, HSQC and HMBC spectra for complexes **1a**, **2a**, **3a**, **5a**, **1b**, **2b**, and **6c**. Microbial activity of ruthenium complexes: Experimental, Figure 1 and Table 1. Crystal and refinement data for complexes **1b**, **2a-CH<sub>2</sub>Cl<sub>2</sub>** and **3b** (Table 2). X-ray crystallographic files in CIF format. CCDC reference numbers 937041–937043 for **1b**, **2a-CH<sub>2</sub>Cl<sub>2</sub>** and **3b**. See DOI: 10.1039/b000000x/

- <sup>1</sup> (a) F. Mendes, M. Groessl, A. A. Nazarov, Y. O. Tsybin, G. Sava, I. Santos, P. J. Dyson, A. Casini, *J. Med. Chem.*, 2011, **54**, 2196–2206; (b) P. C. A. Bruijninx, P. J. Sadler, *Current Opinion in Chemical Biology*, 2008, **12**, 197–206.
- <sup>2</sup> (a) A. C. Komor, J. K. Barton, *Chem. Commun.*, 2013, **49**, 3603–3710; (b) A. A. Yadav, D. Patel, X. Wu, B. B. Hasinoff, *J. Inorg. Biochem.*, 2013, **126**, 1–6; (c) T. Mihály, M. Garijo-Añorbe, F. M. Alberti, P. J. Sanz-Miguel, B. Lippert, *Inorg. Chem.*, 2012, **51**, 10437–10446; (d) K. J. Kilpin, C. M. Clavel, F. Edfæ, P. J. Dyson, *Organometallics*, 2012, **31**, 7031–7039; (e) W. H. Ang, A. Casini, G. Sava, P. J. Dyson, *J. Organomet. Chem.*, 2011, **696**, 989–998; (f) A. Casini, C. G. Hartinger, A. A. Nazarov, P. J. Dyson, *Top Organomet. Chem.*, 2010, **32**, 57–80; (g) A. M. Pizarro, A. Habtemariam, P. J. Sadler, *Top Organomet. Chem.*, 2010, **32**, 21–56.
- <sup>3</sup> (a) B. S. Howerton, Heidary, D. K.; Glazer, E. C. *J. Am. Chem. Soc.*, 2012, **134**, 8324–8327; (b) J. Ruiz, V. Rodriguez, N. Cutillas, A. Espinosa, M. J. Hannon *Inorg. Chem.*, 2011, **50**, 9164–9171; (c) H. Xu, Q.-Q. Zhu, J. Lu, X.-J. Chen, J. Xiao, Z.-G. Liu, S.-P. Chen, M.-L. Tong, L.-N. Ji, Y. Liang, *Inorg. Chem. Commun.*, 2010, **13**, 2010; (d) A. Bergamo, A. Masi, P. J. Dyson, G. Sava, *Int. J. Oncol.*, 2008, **33**, 1281–1289; (e) A. Casini, C. Gabbiani, F. Sorrentino, M. P. Rigobello, A. Bindoli, T. J. Geldbach, A. Marrone, N. Re, C. G. Hartinger, P. J. Dyson, L. Messori, *J. Med. Chem.*, 2008, **51**, 6773–6781; (f) T. Bugarcic, O. Novakova, A. Halamikova, L. Zerkankova, O. Vrana, J. Kasparkova, A. Habtemariam, S. Parsons, P. J. Sadler, V. Brabec, *J. Med. Chem.*, 2008, **51**, 5310–5319; (g) M. A. Jakupc, M. Galanski, V. B. Arion, C. G. Hartinger, B. K. Keppler, *Dalton Trans.*, 2008, 183–194; (h) W. H. Ang, P. J. Dyson, *Eur. J. Inorg. Chem.*, 2006, 4003–4018; (i) M. J. Clarke *Coord. Chem. Rev.*, 2003, **236**, 209–233.
- <sup>4</sup> (a) F. Lentz, A. Drescher, A. Lindauer, M. Henke, R. A. Hilger, C. G. Hartinger, M. E. Scheules, C. Ditrich, B. K. Keppler, U. Jachde, *Anticancer Drugs*, 2009, **20**, 97–103; (b) C. G. Hartinger, S. Zorbas-Seifried, M. A. Jakupc, B. Kynast, H. Zorbas, B. K. Keppler, *J. Inorg. Biochem.*, 2006, **100**, 891–904; (c) J. M. Rademaker-Lakhai, D. van den Bongard, D. Pluim, J. H. Beijnen, J. H. M. Schellens, *Clin. Cancer Res.*, 2004, **10**, 3717–3727.
- <sup>5</sup> For recent studies on RAPTA complexes see: (a) L. Hajji, C. Saraiba-Bello, A. Romerosa, G. Segovia-Torrente, M. Serrano-Ruiz, P. Bergamini, A. Canella, *Inorg. Chem.*, 2011, **50**, 873–882; (b) C. Rios-Luci, L. G. León, A. Mena-Cruz, E. Pérez-Roth, P. Lorenzo-Luis, A. Romerosa, J. M. Padrón, *Bioorg. Med. Chem. Lett.*, 2011, **21**, 4568; (c) W. Kandlioller, C. G. Hartinger, A. A. Nazarov, J. Kasser, R. John, M. A. Jakupc, V. B. Arion, P. J. Dyson, B. K. Keppler, *J. Organomet. Chem.*, 2009, **694**, 922–929; (d) M. H. Garcia, T. S. Moraes, P. Florindo, M. F. M. Piedade, V. Moreno, C. Ciudad, V. Noe, *J. Inorg. Biochem.*, 2009, **103**, 354–361; (e) A. K. Renfrew, A. D. Phillips, A. E. Egger, C. G. Hartinger, S. S. Bosquain, A. A. Nazarov, B. K. Keppler, L. Gonsalvi, M. Peruzzini, P. J. Dyson, *Organometallics*, 2009, **28**, 1165–1172; (f) C. Scolaro, C. G. Hartinger, C. S. Allardyce, B. K. Keppler, P. J. Dyson, *J. Inorg. Biochem.*, 2008, **102**, 1743–1748; (g) T. Bugarcic, A. Habtemariam, J. Stepankova, P. Heringova, J. Kasparkova, R. J. Deeth, R. D. L. Johnstone, A. Prescimone, A. Parkin, S. Parsons, V. Brabec, P. J. Sadler, *Inorg. Chem.*, 2008, **47**, 11470–11486; (h) C. A. Vock, A. K. Renfrew, R. Scopelliti, L. Juillierat-Jeanerret, P. J. Dyson, *Eur. J. Inorg. Chem.*, 2008, 1661–1671.
- <sup>6</sup> (a) A. García-Fernández, J. Díez, A. Manteca, J. Sánchez, R. García-Nava, B. G. Sierra, F. Mollinedo, M. P. Gamasa, E. Lastra, *Dalton Trans.*, 2010, **39**, 10186–10196; (b) A. García-Fernández, J. Díez, A. Manteca, J. Sánchez, M. P. Gamasa, E. Lastra, *Polyhedron*, 2008, **27**, 1214–1228.
- <sup>7</sup> (a) D. Cuervo, J. Díez, M. P. Gamasa, J. Gimeno, *Organometallics*, 2005, **24**, 2224–2232; (b) J. Díez, M. P. Gamasa, J. Gimeno, P. Paredes, *Organometallics*, 2005, **24**, 1799–1802; (c) D. Cuervo, M. P. Gamasa, J. Gimeno, *J. Mol. Catal. A*, 2006, **249**, 60–64; (d) P. Paredes, J. Díez, M. P. Gamasa, *J. Organomet. Chem.*, 2008, **693**, 3681–3687; (e) M. Panera, J. Díez, M. P. Gamasa, *Inorg. Chem.*, 2006, **45**, 10043–10045; (f) M. Panera, J. Díez, I. Merino, E. Rubio, M. P. Gamasa, *Inorg. Chem.*, 2009, **48**, 11147–11160.
- <sup>8</sup> (a) D. Cuervo, M. P. Gamasa, J. Gimeno, *Chem. Eur. J.*, 2004, **10**, 425–432; (b) P. Paredes, J. Díez, M. P. Gamasa, *Organometallics*, 2008, **27**, 2597–2607; (c) D. Cuervo, E. Menéndez-Pedregal, J. Díez, M. P. Gamasa, *J. Organomet. Chem.*, 2011, **696**, 1861–1867.
- <sup>9</sup> (a) H. M. Er, T. W. Hambley, *J. Inorg. Biochem.*, 2009, **103**, 168–173; (b) C. I. Diakos, M. Zhang, P. J. Bale, R. R. Fenton, T. W. Hambley, *Eur. J. Med. Chem.*, 2009, **44**, 2807–2814; (c) A. M. Montaña, F. J. Bernal, J. Lorenzo, C. Farnós, C. Batalla, M. J. Priet, V. Moreno, F. X. Avilés, J. M. Mesas, M. T. Alegre, *Biorg. Med. Chem.*, 2008, **16**, 1721–1737; (d) J. Malina, M. Vojtiskova, V. Brabec, C. I. Diakos, T. W. Hambley, *Biochem. Biophys. Res. Commun.*, 2005, **332**, 1034–1041; (e) O. Delalande, J. Malina, V. Brabec, J. Kozelka, *Biophys. J.*, 2005, **88**, 4159–4169; (f) R. R. Fenton, W. J. Easdale, N. M. Er, S. M. O'Mara, M. J. McKeage, P. J. Russell, T. W. Hambley, *J. Med. Chem.*, 1997, **40**, 1090–1098; (g) F. P. Fanizzi, F. P. Intini, G. Maresca, G. Natile, R. Quaranta, M. Coluccia, L. Di Bari, D. Giordano, M. A. Mariggio, *Inorg. Chim. Acta*, 1987, **137**, 45–51; (h) M. Noji, K. Okamoto, Y. Kidani, T. Tashiro, *J. Med. Chem.*, 1981, **24**, 508–514; (i) Y. Kidani, K. Inagaki, M. Iigo, A. Hoshi, K. Kureitani, *J. Med. Chem.*, 1978, **21**, 1315–1318.
- <sup>10</sup> C. A. Puckett, J. K. Barton, *Biochemistry*, 2008, **47**, 11711–11716.
- <sup>11</sup> (a) C. W. Jiang, *J. Inorg. Biochem.*, 2004, **98**, 497–501; (b) D. Z. M. Coggan, I. S. Haworth, P. J. Bates, A. Robinson, A. Rodger, *Inorg. Chem.*, 1999, **38**, 4486–4497; (c) P. Lincoln, A. Broo, B. Nordén, *J. Am. Chem. Soc.*, 1996, **118**, 2644–2653; (d) C. Hiort, P. Lincoln, B. Nordén, *J. Am. Chem. Soc.*, 1993, **115**, 3448–3454; (e) M. Eriksson, M. Leijon, C. Hiort, B. Norden, A. Gräslund, *Biochemistry*, 1994, **33**, 5031–5040; (f) S. Aatyanarayana, J. C. Dabrowiak, J. B. Chaires, *Biochemistry*, 1992, **31**, 9319–9324; (g) J. K. Barton, J. M. Goldberg, C. V. Kumar, N. J. Turro, *J. Am. Chem. Soc.*, 1986, **108**, 2081–2088; (h) J. K. Barton, A. T. Danishefsky, J. M. Goldberg, *J. Am. Chem. Soc.*, 1984, **106**, 2172–2176.
- <sup>12</sup> (a) A. D. Phillips, L. Gonsalvi, A. Romerosa, F. Vizza, M. Peruzzini, *Coord. Chem. Rev.*, 2004, **248**, 955–993; (b) J. Bravo, S. Bolaño, L. Gonsalvi, M. Peruzzini, *Coord. Chem. Rev.*, 2010, **254**, 555–607.
- <sup>13</sup> The pattern of  $^1\text{H}$  and  $^{13}\text{C}\{^1\text{H}\}$  NMR spectra of pybox ligands provides unequivocal structural elucidation for either *cis* and *trans* dihalogen octahedral complexes. See for example *cis*- and *trans*-[RuCl<sub>2</sub>(L)(R-pybox)] (L = Phosphane) (ref. 8a).

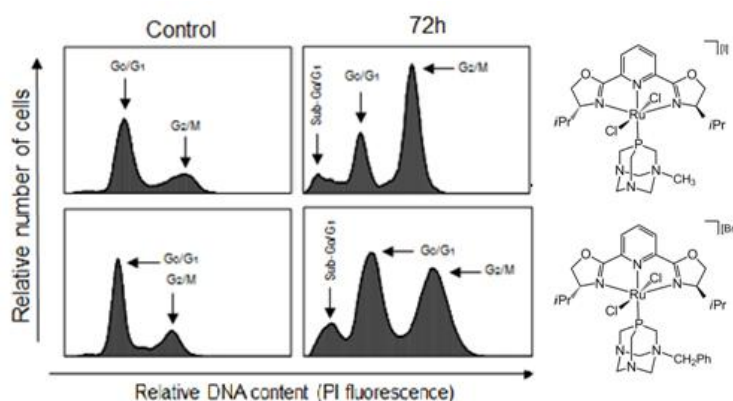
- <sup>14</sup> (a) C. A. Mebi, P. N. Radhika, B. J. Frost, *Organometallics*, 2007, **26**, 429–438; (b) A. Romerosa, M. Saoud, T. Campos-Malpartida, C. Lidrissi, M. Serrano-Ruiz, M. Peruzzini, J. A. Garrido-Cárdenas, F. García-Maroto, *Eur. J. Inorg. Chem.*, 2007, **45**, 2803–2812; (c) A. Romerosa, T. Campos-Malpartida, C. Lidrissi, M. Saoud, M. Serrano-Ruiz, M. Peruzzini, J. A. Garrido-Cárdenas, F. García-Maroto, *Inorg. Chem.*, 2006, **45**, 1289–1298.
- <sup>15</sup> W. Geary, *J. Coord. Chem. Rev.*, 1971, **7**, 81–122.
- <sup>16</sup> A. García-Fernández, J. Díez, M. P. Gamasa, E. Lastra, *Inorg. Chem.*, 2009, **48**, 2471–2481.
- <sup>17</sup> V. Cadierno, M. P. Gamasa, J. Gimeno, L. Iglesias, S. García-Granda, *Inorg. Chem.*, 1999, **38**, 2874–2879.
- <sup>18</sup> T. Steiner, *Angew. Chem. Int. Ed.*, 2002, **41**, 48–76.
- <sup>19</sup> J. J. Biemer, *Ann. Clin. Lab. Sci.* 1973, **3**, 135–140.
- <sup>20</sup> C. Gajate, I. Barasoain, J. M. Andreu, F. Mollinedo, *Cancer Res.*, 2000, **60**, 2651–2659.
- <sup>21</sup> F. Mollinedo, C. Gajate, *Apoptosis*, 2003, **8**, 413–450.
- <sup>22</sup> M. A. Bennet, A. K. Smith, *J. Chem. Soc., Dalton Trans.*, 1974, 233–241.
- <sup>23</sup> H. Nishiyama, Y. Itoh, H. Matsumoto, S. B. Park, K. Itoh, *J. Am. Chem. Soc.*, 1994, **116**, 2223–2224.
- <sup>24</sup> H. Nishiyama, M. Kondo, T. Nakamura, K. Itoh, *Organometallics*, 1991, **10**, 500–508.
- <sup>25</sup> D. J. Daigle, *Inorg. Synth.*, 1998, **32**, 40–45.
- <sup>26</sup> *CrysAlis<sup>Pro</sup> CCD, CrysAlis<sup>Pro</sup> RED*. Oxford Diffraction Ltd., Abingdon, Oxfordshire, UK. 2008.
- <sup>27</sup> L. J. Farrugia, *J. Appl. Crystallogr.* 1999, **32**, 837–838.
- <sup>28</sup> P. T. Beurskens, G. Admiraal, G. Beurskens, W. P. Bosman, S. García-Granda, R. O. Gould, J. M. M. Smits, C. Smykalla, *The DIRDIF Program System*; Technical Report of the Crystallographic Laboratory; University of Nijmegen: Nijmegen, The Netherlands, 1999.
- <sup>29</sup> A. Altomare G. Cascarano, C. Giacovazzo, A. Gualardi, M. C. Burla, G. Polidori, M. Camalli, *J. Appl. Cryst.*, 1994, **27**, 435–436.
- <sup>30</sup> G. M. Sheldrick, *SHELXL97: Program for the Refinement of Crystal Structures*; University of Göttingen: Göttingen, Germany, 2008.
- <sup>31</sup> A. L. Spek, *PLATON: A Multipurpose Crystallographic Tool*; University of Utrecht, The Netherlands, 2007.
- <sup>32</sup> *Tables for X-Ray Crystallography*; Kynoch Press; Birmingham, U.K., 1974; Vol. IV (present distributor: Kluwer Academic Publishers; Dordrecht, The Netherlands).
- <sup>33</sup> PARST M. Nardelli, *Comput. Chem.* 1983, **7**, 95–98.
- <sup>34</sup> CCDC numbers 937041–937043 contain the crystallographic information for **1b**, **2a**·CH<sub>2</sub>Cl<sub>2</sub> and **3b**.
- <sup>35</sup> C. Gajate, A. M. Santos-Beneit, A. Macho, M. C. Lázaro, A. Hernández-DeRojas, M. Modolell, E. Muñoz, F. Mollinedo, *Int. J. Cancer*, 2000, **86**, 208–218.

# Antitumor Activity of New Enantiopure Pybox-Ruthenium Complexes

View Article Online  
DOI: 10.1039/C3DT51160J

Estefania Menéndez-Pedregal,<sup>a</sup> Josefina Díez,<sup>a</sup> Ángel Manteca,<sup>b</sup> Jesús Sánchez,<sup>b</sup> Ana C. Bento,<sup>c</sup> Rósula García-Navas,<sup>c</sup> Faustino Mollinedo,<sup>c</sup> M. Pilar Gamasa<sup>\*a</sup> and Elena Lastra<sup>\*a</sup>.

## Graphical Abstract



New water-soluble ruthenium complexes containing enantiopure pybox ligands have been synthesized and their interactions with plasmidic DNA and cytotoxic activity against the human cervical cancer HeLa cell line studied.